Spacelike Geodesics and Other Puzzles in the Mixmaster Universe

KENWAY, ANGHARAD,SONIA

Spacelike Geodesics and Other Puzzles in the Mixmaster Universe

Angharad Sonia Kenway

A Thesis presented for the degree of
Doctor of Philosophy

Centre for Particle Theory
Department of Mathematical Sciences
University of Durham
England

October 2011

Dedicated to

my family

Spacelike Geodesics and Other Puzzles in the Mixmaster Universe

Angharad Sonia Kenway

Submitted for the degree of Doctor of Philosophy
October 2011

Abstract

In this thesis we are going to investigate the behaviour of geodesics in a metric with a singularity known as the "Mixmaster Universe". This was motivated from previous work done, where the now well-known AdS/CFT correspondence was used to extract information about an AdS Schwarzschild black hole singularity beyond the horizon by studying correlators on the boundary that correspond to spacelike geodesics which bounce off the singularity. It was then shown that when the singularity was a cosmological one (in this case a Friedmann Robertson Walker cosmology with a Big Crunch), this was no longer possible as it is impossible for spacelike geodesics to bounce off this kind of singularity. This raises the question of whether, when an example of a more general singularity (the "Mixmaster Universe") is considered, it is possible for the spacelike geodesics to bounce away from this kind of singularity. This would enable us to potentially extract information about the singularity from the boundary correlators. Unfortunately, it will be shown that bouncing of such geodesics is extremely unlikely (if not impossible) and thus we would be unable to extract information about the singularity in the mixmaster universe using such a technique. We also discuss another aspect of the evolution of the mixmaster universe which shows that it does indeed have a very complicated evolution.

Declaration

The work in this thesis is based on research carried out at the Centre for Particle Theory, Department of Mathematical Sciences, Durham University, England. No part of this thesis has been submitted elsewhere for any other degree or qualification and it is all my own work unless referenced to the contrary in the text.

Acknowledgements

It is a long and difficult road to a PhD and it is a journey that would not have been possible without the help of many people. Firstly, thanks goes to my supervisor Veronika Hubeny for all her help and guidance over the four years. I would also like to thank all the students and staff in the Maths Department for the many lively discussions we have had over coffee throughout the years on every possible subject. Thanks to all my family for its support especially in the last few stressful days of writing this thesis and thanks to all my friends around Durham (and beyond) for all the great times we have had in the last four years when I wasn't in the office working. An honourable mention goes to "Team Sporcle" for helping me learn so much general knowledge trivia outside the world of maths and physics. I'm sure that the knowledge of all the US state capitals, presidents and countries of the world will be invaluable one day.

Contents

List of Figures

List of Tables

Chapter 1

Introduction

Einstein's General Theory of Relativity [1] is the most widely accepted theory of the gravitational force. The fundamental principle of general relativity (GR) is that the gravitational force is caused by curvature in space-time itself and that this curvature is in turn caused by the matter within the space-time. This is represented simply and elegantly through Einsteins' equations:

$$G_{\mu\nu} = 8\pi G_N T_{\mu\nu} \tag{1.1}$$

where $G_{\mu\nu}$ is called the Einstein tensor and encodes the curvature (i.e. the metric) of space-time and $T_{\mu\nu}$ is the stress energy tensor and contains information about matter in the space-time (G_N is Newton's constant). This view of gravity is not only extremely elegant but its results have been verified through many experimental observations and lead us to accept that it is the correct view of gravity. Nevertheless, there are many solutions of Einstein's equations which contain singularities, such as those of black holes or a big bang scenarios. Singularities are areas of space-time where the theory of general relativity breaks down. But we would still like to be able to study such singularities in theoretical. Specifically in this thesis, we are aiming to study a metric known as the "mixmaster universe" which exhibits extremely complex behaviour near its singularity (this will be explained in greater detail in chapter 2). However, this is impossible to do in the classical formulation of general relativity. Instead we are going to use the more recently developed string theory and the associated AdS/CFT correspondence to examine singularities. Both

string theory and the AdS/CFT correspondence are large subjects with a somewhat daunting amount of literature available on both but we are going to have to discuss them a little further to motivate our study of the mixmaster universe. We will briefly discuss the development of string theory using [2–4] as our principle sources then we will give an overview of the AdS/CFT correspondence. In the second section of this chapter, we will discuss precisely how we can use the AdS/CFT correspondence to study singularities in a gravitational theory.

1.1 A Short Introduction to String Theory and the AdS/CFT Correspondence

One of the goals of theoretical physics in recent times has been to unify all the forces of nature into one theory, a so-called "theory of everything". Currently there are two well-tested theories, the aforementioned general theory of relativity for gravity (which is a classical theory) and the quantum field theories used to describe the electroweak and strong interactions of fundamental particles in the Standard Model. Both of these theories have been extremely successful in their respective regimes. General relativity can be used to describe "large scale" problems where quantum effects are minimal and quantum theories describe "small scale" problems in which gravity is negligible. But it remains that they are inconsistent. One could ask why (if these theories are so successful) should we expect them to be unified into one? There are two reasons in my opinion. Firstly, from the historical perspective that over time we have successfully united the other forces initially believed to be different, such as Maxwell's unification of electricity and magnetism and the Weinberg-Salam model of the 1960s which unified electromagnetism and the weak nuclear force (into the electro-weak force), as well as the intuitive notion that leads one to expect our universe to have one theory governing its behaviour and interactions. Secondly, and a stronger argument, is the fact that there are some situations such as times near the Big Bang and black holes where both gravity and quantum effects are heavily present and thus we require a quantum theory of gravity to study these. Indeed, as mentioned above, it is the study of such situations which is the

main motivation for the work in this thesis.

Attempts to unite these theories have been many but so far the (arguably) most promising candidate is string theory.

1.1.1 String Theory

String theory, famously, is a completely new way of thinking about the fundamental particles of nature. Particles in Quantum Field Theories (QFTs) are treated as zero-dimensional points. In string theory however, the fundamental objects are extended (i.e. one-dimensional strings) and the different particles correspond to different vibrational modes of the string. One of these vibrational modes is a spin-2 particle, the graviton, and thus the theory contains gravity. Strings in string theory can be open (have end points) or closed (no endpoints). This theory, not only elegantly unites all four fundamental forces but does so while providing a theory of quantum gravity which is UV finite in perturbation theory. Another advantage is the massive reduction of arbitrary dimensionless parameters. The Standard Model has about twenty parameters whereas string theory reduces this to just one.

However, as a theory of our physical world, it is not without its difficulties. While we have been referring to "string theory", there are actually many different string theories that have been found and studied. The first string theory describing only bosonic strings, required 26 space-time dimensions and predicted a particle with negative mass squared (a tachyon) which is clearly a problem in a four dimensional world full of fermions (and no tachyons).

Fermions were introduced by formulating "superstring" theory, a supersymmetric string theory which had fermionic strings as well as bosonic ones (supersymmetry being a symmetry which connects bosons to fermions). Supersymmetry also helped get rid of the tachyon in the theory. This led to five consistent superstring theories with 10 space-time dimensions: types I, IIA, IIB and the heterotic string theories

known via their gauge groups $SO(32)$ and $E_8 \times E_8$. These still have more dimensions than required but these extra dimensions can be dealt with by compactifying them and it is interesting to note that, while there are too many dimensions, the number of dimensions in string theory emerges from the theory whereas in the Standard Model the fact that there are four space-time dimensions has to be inserted in the theory *a priori*. Further studies of of these string theories in the 1990s uncovered dualities between them suggesting they were all different manifestations of one unique theory known as "M-theory". Further work led to the discovery of D-branes, most simply described as extended objects on which the ends of open strings are constrained to move. This in turn opened a path leading to the formulation of the AdS/CFT correspondence. The AdS/CFT correspondence conjectures that there exists a duality between a gauge (i.e. field) theory and a string theory living in one dimension higher.

1.1.2 The AdS/CFT Correspondence

Considering the excitations of D3-branes led to the following statement of the AdS/CFT conjecture in [5] as:

"$\mathcal{N} = 4$ SU(N) Super-Yang-Mills (SYM) theory in 3+1 dimensions is the same as (or dual to) type IIB superstring theory on $AdS_5 \times S^5$"

So what does this statement mean? On one side of the correspondence we have $\mathcal{N} = 4$ Super-Yang-Mills theory which is a non-abelian supersymmetric gauge theory in 4 dimensions (with gauge group SU(N)). It is a conformal field theory which means it is invariant under scale transformations $x^\mu \to \lambda x^\mu$. On the other side of the correspondence we have a gravitational theory in AdS (Anti de Sitter) space. AdS space is a maximally symmetric solution of Einstein's equations with constant negative curvature. So we have a relation between a four dimensional field theory and a five dimensional gravitational theory. While the original derivation of this correspondence was formulated via the study of excitations of D-branes, it was demonstrated by Horowitz and Polchinski in [7] that it can also be motivated with-

out the need for string theory and can be justified using only knowledge about gauge theories and gravity. Their assertion was as follows:

"Hidden within every non-Abelian gauge theory [...] is a theory of quantum gravity"

This was demonstrated as follows. The "holographic principle" of 't Hooft [8] and Susskind [9] suggests that any gravitational theory should be related to a non-gravitational theory in one fewer dimensions. So, if we want to find a gravitational theory in our gauge theory, we are going to have to find both a graviton and an extra dimension encoded in it. The gauge theory being considered will be a Yang-Mills gauge theory and so have gauge group $SU(N)$). Suppose (with some foresight) we take this extra dimension to be the energy scale of the gauge theory. In addition we are going to require that

1. N is large to account for the larger number of degrees of freedom in the higher dimensional theory.

2. The coupling of the theory is strong so that the theory is strongly quantum mechanical as classical general relativity nothing like classical Yang-Mills theory.

3. Supersymmetry without which the second requirement will cause the theory to be highly unstable.

With this in mind, we consider the most supersymmetric theory $\mathcal{N} = 4$ SYM gauge theory. This theory benefits from the fact that the $\mathcal{N} = 4$ supersymmetry makes the coupling strong and constant for a large range of energies. So as we are considering our energy range as the fifth dimension we are seeking, this allows us to have a large fifth dimension. It also means that the theory is conformal (invariant under scale transformations). Under the scale transformation $x^\mu \to \lambda x^\mu$ for the spatial coordinates, the energy scale r say, should transform inversely i.e. $r \to r/\lambda$. So if we seek a five dimensional metric which is invariant in these scale transformations and also under the usual Poincaré symmetries, then we find the most general metric

is given by:

$$ds^2 = \frac{r^2}{l^2}\eta_{\mu\nu}dx^\mu dx^\nu + \frac{l^2}{r^2}dr^2 \tag{1.2}$$

where l is a constant and $\eta_{\mu\nu} =$ is the Minkowski metric tensor. This is in fact the metric of AdS_5. So we have found what we wanted at the start. While this is a fairly rough argument, it does seem to strongly imply that the gauge theory does seem to be equivalent to a gravitational theory with one more dimension.

So now that we appear to have a duality between a field theory and a gravitational theory, it makes sense to consider the field theory as living on the boundary of the gravitational theory. This is where the notion of holography comes from. Through this correspondence we can study the bulk space-time by studying a field theory in a smaller number of dimensions on the boundary (which is analogous to an optical hologram where a three dimensional image is produced from a two dimensional one).

Conversely, it can also be used the other way - studying the gravitational theory can yield results about the field theory. For example, the discovery in [10] that a thermal state in $\mathcal{N} = 4$ SYM is equivalent to a large mass AdS-Schwarzschild black hole has led to many new applications of the AdS/CFT correspondence in the studies of superconductivity and superfluidity (for details see [11, 12]). Features of superconductors for example, can be derived through the correspondence from the thermodynamic properties of the black hole.

Nevertheless, despite having a considerable amount of evidence in its favour, it is important to note that the correspondence is, at this time, still a conjecture and a full proof has yet to be found.

1.2 Probing Singularities

We are now going to review the work of [13] and [14] in more detail to motivate our study of the mixmaster universe by firstly looking at other singularities. Singularities are places in a metric where the theory of general relativity breaks down and we need a quantum theory of gravity to study these regions of spacetimes. Because, according to the holographic principle, the full theory of the bulk spacetime must be encoded in the field theory on the boundary then this means that the singularity must be encoded in the field theory as well. It may then be possible to use the aforementioned AdS/CFT correspondence between string theory in asymptotically $AdS_5 \times S_5$ spacetimes and four dimension $\mathcal{N} = 4$ SYM theory to have a closer look at such singularities. Often such singularities are hidden behind event horizons. These are hypersurfaces where any timelike curve beyond the event horizon has the singularity in its future and cannot escape to infinity. This means that there is no way in classical GR to look inside event horizons. Much work has been done on finding ways to extract information from behind an event horizon via the boundary correlators [15–18]. It was shown in [18] that by using the AdS/CFT correspondence and studying the correlators on the boundary, one can probe inside the event horizon of a three dimensional BTZ black hole.

The set-up is such that we have two operators, one on each of the asymptotic boundaries so these are operators in the conformal field theory side of the correspondence. Each of these is dual to a large mass scalar field in the bulk (the AdS side). We can then want to calculate the 2 point correlation function in the field theory which can be done by calculating the propagator in the bulk. This is done by summing over the paths between these two points where each path gives a contribution of $e^{-m\mathcal{L}}$ to the propagator and $\mathcal{L}$ is the proper length of such a path suitably regulated. If we take the limit in which m is large, then this this sum will be dominated by path contributing the smallest $\mathcal{L}$ i.e. the shortest geodesic connecting the two points. So we can approximate the propagator in the bulk by:

$$e^{-m\mathcal{L}} \tag{1.3}$$

where $\mathcal{L}$ is the proper length of the spacelike geodesic joining the two points on the boundary where we have placed the operators. This propagator in the bulk is then dual to correlation function in the CFT on the boundary. As it is possible for the geodesic to pass through parts of the metric inside the event horizon, this implies that aspects of the geometry from beyond the event horizon must be encoded in the correlators on the boundary. This implies that in terms of the AdS/CFT correspondence, a singularity in the spacetime leaves a signature in the dual field theory. So turning this problem around, it should be possible to study singularities via studying appropriate field theory correlators in the CFT.

In [13], a higher dimensional AdS black hole was considered. It was found that in a five dimensional AdS black hole there are radial spacelike geodesics which bounce off the singularity. Although there were some subtleties that required the correlators to be analytically continued, it was possible to study this singularity by studying the correlators corresponding to these bouncing geodesics. This raises the question of whether it is possible to probe other singularities using this technique.

An attempt was made to apply such a technique to a cosmological singularity with a "Big Crunch" in [14] as it is possible to embed cosmological singularities into an AdS/CFT set-up. This could enable us to use the CFT correlators to probe this cosmological singularity. Unfortunately, this is shown not to be the case as spacelike geodesics cannot bounce off this kind of singularity. As this is shown via similar analysis to what we will use in later chapters to study other metrics we will discuss this example in a little more detail here. To see this we consider a spherically symmetric metric and consider the geodesic equations within this metric. The radial part of the metric is given by:

$$ds^2 = -dt^2 + a^2(t)dr^2 \tag{1.4}$$

To find the geodesic equations (following standard techniques from say [24, 25]), we recast this as a Lagrangian

$$\mathcal{L} = \frac{1}{2}(-\dot{t}^2 + a^2(t)\dot{r}^2) \tag{1.5}$$

where $\dot{}$ means differentiating with respect to τ, the affine parameter of the geodesic. We obtain the t geodesic equation by the Euler Lagrange equations

$$\frac{d}{d\tau}\left(\frac{\partial \mathcal{L}}{\partial \dot{t}}\right) - \frac{\partial \mathcal{L}}{\partial t} = 0 \tag{1.6}$$

to get

$$\ddot{t} + a(t)a'(t)\dot{r}^2 = 0 \tag{1.7}$$

where $'$ means $\frac{d}{dt}$. For a geodesic to bounce off the singularity which is in the future, we require a point along the geodesic where $\dot{t} = 0$ and $\ddot{t} < 0$. The first condition can be satisfied for a spacelike geodesic but the second is more problematic. As $\dot{r}^2$ and $a(t)$ are positive, that means that the satisfaction of this condition is purely dependent on the sign of $a'(t)$. If $a'(t)$ is positive then $\ddot{t}$ is negative and vice versa. If we consider a Friedmann Robertson Walker metric, $a(t)$ is the scale factor of this metric. In this scenario of a future singularity, this means that near the singularity, the space is contracting and hence $a'(t) < 0$. So the spacelike geodesics all have $\ddot{t} > 0$ and hence cannot bounce off the singularity. This means that these geodesics hit the singularity. Note that the same analysis means that neither can spacelike geodesics bounce off a past singularity (Big Bang) in this metric. The reasoning is the same but with opposite signs in the bouncing condition on $\ddot{t}$ and $a'(t)$.

We can also use this analysis for a Schwarzschild black hole. We can do a coordinate transformation that will produce a metric of the same type as in (1.4). This transformation requires us to change the sense of the r and t coordinates. So t will be the radial coordinate and r the time coordinate in the Schwarzschild case. This gives a function $a(t)$ such that near to the singularity $a(t) \sim -\frac{1}{t}$ which makes $a'(t) \sim \frac{1}{t^2}$ so $a'(t) > 0$. This means that we can have geodesics satisfying the conditions that $\ddot{t} < 0$ and $\dot{t} = 0$. As t is the radial coordinate here this shows quickly that we do indeed have radial spacelike geodesics which bounce off the singularity in the black hole scenario.

This means that a cosmological singularity is fundamentally different from the AdS Schwarzschild black hole. We cannot have spacelike geodesics bouncing off a

cosmological singularity of the FRW type and so cannot use the associated correlators in the field theory to investigate the singularity in this way. The main subject of this thesis is to consider a more general type of cosmological singularity (the mixmaster universe) and see if this kind of singularity, with its much more complex behaviour near to the singularity, allows spacelike geodesics to bounce thus giving us the chance to probe this singularity via the field theory in the AdS/CFT correspondence.

1.3 Summary

In this chapter we have attempted to motivate the study of geodesics which bounce off a singularity. We introduced string theory and the AdS/CFT correspondence which allow us to infer information about spacelike geodesics in the bulk via the correlators on the boundary. This has allowed us to probe beyond the event horizon of a black hole using geodesics which bounce off the singularity. We attempted to apply this technique to a cosmological (FRW) singularity and found that in this scenario, there are no bouncing spacelike geodesics. Now we are going to consider a more general cosmological singularity and see if we can find spacelike geodesics which bounce of this singularity thus giving us the opportunity to determine more about this singularity using the AdS/CFT correspondence. In the next chapter we will introduce the mixmaster universe and explain its connection to the Kasner metric. In chapter three, we will then study spacelike geodesics in this Kasner metric to provide us with some tools for modelling the mixmaster universe and its geodesics. Chapters four and five will use some different techniques (both numerical and analytic) to see if it is indeed possible for geodesics to bounce off the singularity. Chapter four will definitively show that in some situations we can show that geodesic bouncing close to the singularity is impossible and chapter five will attempt to determine whether under certain modifications of our model it is possible to rescue the bouncing. In chapter six we then tangentially discuss an interesting feature about the mixmaster universe which was discovered while investigating this geodesic problem. This demonstrates some other interesting and complex features

of the mixmaster universe and demonstrated that this cosmology has very intricate behaviour making its study problematic.

Chapter 2

Background

In this chapter we are going to introduce the main subject of interest in this thesis, the mixmaster universe. In order to properly discuss the mixmaster universe, it is going to be useful to first introduce some facts about the Kasner metric, a description of which is found in [19] among many other places.

2.1 The Kasner Metric

The Kasner metric is homogeneous and anisotropic and is given by

$$ds^2 = -dt^2 + t^{2p_1}dx_1^2 + t^{2p_2}dx_2^2 + t^{2p_3}dx_3^2 \tag{2.1}$$

where the $\{p_i\}$ are constants. It can be shown that in order for this metric to satisfy Einstein's equations in a vacuum given by:

$$R_{\mu\nu} = 0 \tag{2.2}$$

where $R_{\mu\nu}$ is the Ricci curvature tensor, we must have that:

$$p_1 + p_2 + p_3 = p_1^2 + p_2^2 + p_3^2 = 1 \tag{2.3}$$

Firstly note there is the "obvious" solution set of $\{1, 0, 0\}$ and its permutations but it can be shown that this is simply Minkowski space under a change of coordinates and therefore doesn't have a singularity at $t = 0$. The other solutions do have a singularity at $t = 0$. Secondly, note that the first condition describes a plane and

the second describes a sphere. So the set of constants satisfying these conditions is the circle where these intersect (illustrated in figure 2.1).

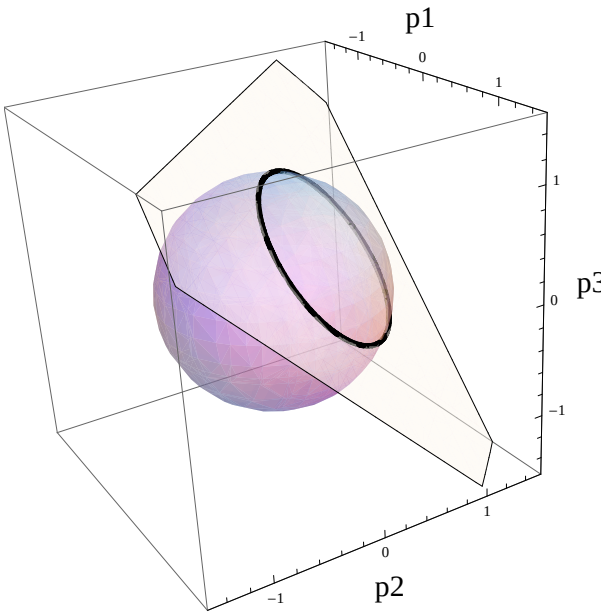

Figure 2.1: A plot of the circle of parameters $\{p_1, p_2, p_3\}$ which satisfy the conditions for the Kasner metric.

We can also see that these conditions require one of the constants to be negative. Without loss of generality, we will take this to be p_1 and from equation (2.3), we can see that this gives us:

$$-\frac{1}{3} \leq p_1 \leq 0 \tag{2.4}$$

while p_2 and p_3 then lie between 0 and $\frac{2}{3}$. The negative value of p_1 means that the metric is contracting in this direction (and expanding in the other two) although the volume element

$$\sqrt{-g} = t^{p_1+p_2+p_3} = t \tag{2.5}$$

is constantly increasing so this is an expanding universe.

It should also be noted, however, that three parameter with two constraints means that only one of them is independent. Thus these constants can therefore be written in terms of one parameter. A useful parametrisation which we will use for

the remainder of this thesis is that of the Khalatnikov-Lifschitz parameter u, where the set $\{p_i\}$ are given by:

$$\begin{aligned} p_1 &= \frac{-u}{1+u+u^2} \\ p_2 &= \frac{1+u}{1+u+u^2} \\ p_3 &= \frac{u(1+u)}{1+u+u^2} \end{aligned} \tag{2.6}$$

It is also useful to observe at this stage from [20], the following identities of the parametrisation (2.6), namely that:

$$\begin{aligned} p_1\left(\frac{1}{u}\right) &= p_1(u) \\ p_2\left(\frac{1}{u}\right) &= p_3(u) \\ p_3\left(\frac{1}{u}\right) &= p_2(u) \end{aligned} \tag{2.7}$$

so we can always take $u > 1$.

This gives us some useful facts about Kasner metrics which will be required when we are discussing the mixmaster universe in the next section.

2.2 The Mixmaster Universe

The mixmaster universe arose from work done by Belinsky, Khalatnikov and Lifschitz, to find a general solution to Einstein's equations with a singularity [20–22]. Here we summarise the main results of that work which are required for our model. Their investigations led to a class of solutions representing generalisations of the homogeneous Kasner metric discussed in the previous section. The general solutions found had the form:

$$ds^2 = -dt^2 + (a^2 l_\alpha l_\beta + b^2 m_\alpha m_\beta + c^2 n_\alpha n_\beta) dx^\alpha dx^\beta \tag{2.8}$$

Einsteins' equations in a vacuum ($R_{\mu\nu} = 0$) for this metric give us the following set of equations for a, b and c,

$$\begin{aligned} R_0^0 &= \frac{a''}{a} + \frac{b''}{b} + \frac{c''}{c} = 0 \\ R_l^l &= \frac{(a'bc)'}{abc} + \frac{\lambda^2 a^2}{2b^2c^2} = 0 \\ R_m^m &= \frac{(ab'c)'}{abc} - \frac{\lambda^2 a^2}{2b^2c^2} = 0 \\ R_n^n &= \frac{(abc')'}{abc} - \frac{\lambda^2 a^2}{2b^2c^2} = 0 \end{aligned} \tag{2.9}$$

(where $'$ denotes differentiation with respect to t). Here the quantity λ is defined by:

$$\lambda := \frac{\mathbf{l} \cdot \nabla \times \mathbf{l}}{\mathbf{l} \cdot \mathbf{m} \times \mathbf{n}} \tag{2.10}$$

with similar quantities μ and ν defined by $\mu := \frac{\mathbf{m} \cdot \nabla \times \mathbf{m}}{\mathbf{l} \cdot \mathbf{m} \times \mathbf{n}}$ and $\nu := \frac{\mathbf{n} \cdot \nabla \times \mathbf{n}}{\mathbf{l} \cdot \mathbf{m} \times \mathbf{n}}$. Taking only the leading order terms of these equations gives us a, b, c as

$$\begin{aligned} a &= t^{p_1} \\ b &= t^{p_2} \\ c &= t^{p_3} \end{aligned} \tag{2.11}$$

where the p_i satisfy the same relations as those in the Kasner metric (2.3) but here the p_1, p_2, p_3 are, in fact, functions of the space coordinates. However, we also get higher order terms (i.e. higher powers of $1/t$) in these equations as well. We can get rid of these terms if we impose the condition that $\lambda = 0$.

Perturbations around this condition (so if we allow λ to be non zero and not necessarily small) can then be shown to cause the metric to evolve (if we look towards the $t = 0$ singularity) from its original Kasner-like metric (2.8, 2.11) to another Kasner-like metric with a different set of $\{\tilde{p}_i\}$.

This is done via a substitution: $a = e^{\alpha}$, $b = e^{\beta}$, $c = e^{\gamma}$, $dt = abcd\tau$. The equations (2.9) then become:

$$\begin{aligned} \alpha_{\tau\tau} &= -\frac{1}{2}\lambda^2 e^{4\alpha} \\ \beta_{\tau\tau} &= \gamma_{\tau\tau} = \frac{1}{2}\lambda^2 e^{4\alpha} \end{aligned} \tag{2.12}$$

with the initial conditions that at $\tau \to \infty$, $\alpha_\tau = p_1$, $\beta_\tau = p_2$, $\gamma_\tau = p_3$. The solution then shows that eventually the perturbation in λ is damped and the metric becomes another Kasner-like metric with

$$(\tilde{p}_1, \tilde{p}_2, \tilde{p}_3) = \frac{1}{1+2p_1}(-p_1, p_2 + 2p_1, p_3 + 2p_1) \tag{2.13}$$

Or, in terms of the Khalatnikov-Lifschitz parameter u, the perturbation in λ causes the metric to evolve from that of a Kasner-like metric with parameter u, to one with the parameter $u-1$ with an appropriate relabelling of axes. In fact, using (2.6), the new parameters $\tilde{p}_i$ are given by:

$$\begin{aligned} \tilde{p}_1 &= p_2(u-1) \\ \tilde{p}_2 &= p_1(u-1) \\ \tilde{p}_3 &= p_3(u-1) \end{aligned} \tag{2.14}$$

So the contracting direction has swapped from the first direction to the second direction. If we looked further back in time, we would reach another Kasner-like metric with parameter $u-2$ and the contracting direction would swap back again. This would continue $u-3, u-4\ldots$ with the contracting direction swapping between the first two coordinates until we reach the point where our parameter reaches $u-\lfloor u \rfloor$ and drops below 1. Then we can use the relations (2.7) to return to a value of u larger than one. So for this kind of transition, we would have (if u is initially between 1 and 2) $u \to \frac{1}{u-1}$ and the $\{p_i\}$ would evolve as:

$$\begin{aligned} p_1(u) &\to p_3\left(\frac{1}{u-1}\right) \\ p_2(u) &\to p_1\left(\frac{1}{u-1}\right) \\ p_3(u) &\to p_2\left(\frac{1}{u-1}\right) \end{aligned} \tag{2.15}$$

At this point we can see that this will cause another two directions to begin swapping the contracting direction between them. We are going to call each Kasner-like metric a "Kasner epoch" (or simply an "epoch") and each set of epochs where two directions swap between expanding and contracting an "era" (so a new era begins when u drops to a value less than one). The metric evolves through a succession of

these "epochs" and "eras" which condense towards the singularity.

If we make our initial value of u be irrational, then this evolution will continue indefinitely. Conversely, if we started with a rational value of u, this would eventually evolve to a Kasner-like metric where $u = 0$. This corresponds to the set $\{p_i\}$ in that metric being some permutation of $\{0, 1, 0\}$ and hence we have lost our singularity completely. As a short aside, in my opinion the previous statement is not completely obvious but is relatively straightforward to prove and so a brief proof is provided.

Proposition 1 *Such a sequence with an initially rational u will terminate with $u = 0$.*

Proof 1 *Suppose u is rational and hence can be written:*

$$u = M + \frac{m}{n}$$

where $M, m, n \in \mathbf{N}$, $m < n$. Then after N steps:

$$u = \frac{m}{n}$$

which is reset to:

$$u = \frac{n}{m} = K + \frac{k}{m}$$

where $K, k \in \mathbf{N}$ and $k < m$. This eventually evolves to $\frac{m}{k}$. So we are creating a sequence of denominators $n > m > k$ which is a decreasing sequence of natural numbers, which will eventually give us a rational value of u with denominator 1, and so u will then evolve to 0.

So as we look back towards the singularity at $t = 0$, we have an infinite number of these epochs and eras, each with a Kasner-like metric which condense towards the singularity. It is explained in [20] that a large proportion of these epochs will have a large value of u and so the majority of the sets $\{p_1, p_2, p_3\}$ will be very close to $\{0, 0, 1\}$ but will never actually reach these values. This would imply that most of the eras will be very long so two of the axes will be swapping the contracting direction between them for many epochs before another two begin swapping. The

evolution shows some interesting features. Namely that the evolution of the parameter u can be shown to be chaotic, in the sense that small perturbations in its value lead to extremely different evolutions of the constants. The evolution was demonstrated to be truly chaotic by Cornish and Levin in [26] in which they studied the dynamics of this evolution in depth as a chaotic system.

The name "mixmaster universe" came from work done by Misner [23] on one particular kind of these metrics. His analysis was carried out in a different way to that of BKL but was equivalent [20] to studying the case where $\lambda = \mu = \nu =$ constant. The metric considered by Misner is given by

$$ds^2 = -dt^2 + \sum_k (l_k)^2 \sigma_k^2 \tag{2.16}$$

where

$$\begin{aligned} \sigma_1 &= \sin\psi d\theta - \cos\psi \sin\theta d\phi \\ \sigma_2 &= \cos\psi d\theta + \sin\psi \sin\theta d\phi \\ \sigma_3 &= -(d\psi + \cos\theta d\phi) \end{aligned} \tag{2.17}$$

and $0 \leq \psi \leq 4\pi$, $0 \leq \theta \leq \pi$, $0 \leq \phi \leq 2\pi$. In order to describe the evolution of the parameters, l_k in this metric, they were rewritten in terms of another set of parameters β_k given by

$$l_k = Re^{\beta_k} \tag{2.18}$$

where $R = (l_1 l_2 l_3)^{\frac{1}{3}}$. This gives the condition that $\sum_k \beta_k = 0$, so we can choose two independent parameters β_+ and β_- as

$$\begin{aligned} \beta_+ &= \beta_1 + \beta_2 \\ \beta_- &= \frac{1}{\sqrt{3}}(\beta_1 - \beta_2) \end{aligned} \tag{2.19}$$

The evolution of the metric can then be described in terms of the evolution of these parameters $\beta_\pm$, which determine shape of the universe, in terms of the volume Ω where Ω is defined by the identity $R := e^{-\Omega}$. Considering Einstein's equations near to the singularity (which corresponds to $\Omega \to \infty$) gives the differential equation for

$\beta_\pm$ as

$$4 = \left(\frac{d\beta_+}{d\Omega}\right)^2 + \left(\frac{d\beta_-}{d\Omega}\right)^2 + 4\Lambda^{-1}e^{-4\Omega}V(\beta_+, \beta_-) \tag{2.20}$$

and the equation

$$\frac{d(\log(\Lambda)}{d\Omega} = -4\Lambda^{-1}e^{-4\Omega}V(\beta) \tag{2.21}$$

where Λ is defined via these equations. The potential $V(\beta_+, \beta_-)$ can be shown to be given by

$$V(\beta_+, \beta_-) = \frac{1}{3}e^{-4\beta_+} - \frac{4}{3}e^{-\beta_+}\cosh(\sqrt{3}\beta_-) + \frac{2}{3}e^{2\beta_+}(\cosh 2(\sqrt{3}\beta_-) - 1) + 1 \tag{2.22}$$

In this potential, the equipotential lines in the (β_+, β_-)-plane are that of an equilateral triangle. A contour plot of this potential is shown in figure 2.2 where this triangular symmetry can be seen along with the fact that the potential rises steeply as we move away from the origin. We can view our parameters (β_+, β_-) as a point

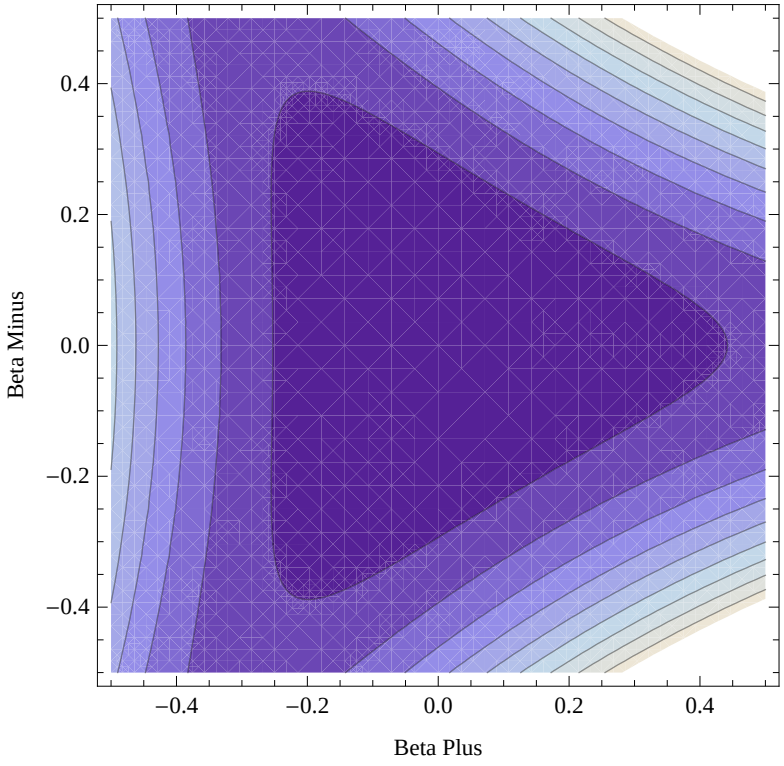

Figure 2.2: A contour plot showing the equipotential lines of the potential $V(\beta_+, \beta_-)$ demonstrating the triangular symmetry of this potential.

moving in this potential. Much of the time, this potential remains small, and so the differential equation (2.20) describes free motion of (β_+, β_-) and when this is

the case, the metric appears to be that of a Kasner metric where the Kasner metric parameters (p_1, p_2, p_3) are given by the relations

$$\begin{aligned} \frac{d\beta_+}{d\Omega} &= 3p_3 - 1 \\ \frac{d\beta_-}{d\Omega} &= \sqrt{3}(p_2 - p_1) \end{aligned} \tag{2.23}$$

However, periodically the point (β_+, β_-) hits one of the walls of the triangular potential and when this happens, the metric shifts from one Kasner model to another at each bounce. Indeed it could be further shown that the amount of time spent in which the point (β_+, β_-) spent bouncing against the potential wall is small compared to the amount of time in free motion. So we can view the shift between two Kasner metrics as occurring comparatively quickly. In [23], the Kasner parameters (2.23) are written in terms of a parameter s, where

$$\begin{aligned} 3p_3 - 1 &= 2\frac{(3 - s^2)}{s^2 + 3} \\ \sqrt{3}(p_2 - p_1) &= 4\frac{(\sqrt{3}s)}{s^2 + 3} \end{aligned} \tag{2.24}$$

and this bouncing can then be written in terms of this parameter as $\frac{1}{3}s \rightarrow \frac{3}{s}$. This is then shown to be equivalent to the evolution of the different parameter $u \rightarrow u - 1$ under some permutations of the Kasner parameters p_i.

So we have found this metric to exhibit the same qualitative behaviour as in the BKL analysis. The metric evolves as a sequence of Kasner-like metrics in which the transition between the metrics occurs comparatively quickly compared to the time spent in each epoch. This motivates us to construct a model which encapsulates this behaviour by matching together a sequence of Kasner metrics whose parameters $p_i(u)$ evolve in the way prescribed by the rule that $u \rightarrow u - 1$.

Misner thought that because this singularity could be shown not to have particle horizons, then it could be a candidate for the "Big Bang" singularity and thus explain the "horizon problem" where areas of the cosmic microwave background which are not causally linked appear to have the same temperature although now this can be explained via inflationary theory. Khalatnikov and Lifschitz also suggested it

could be this kind of singularity in the final stages of gravitational collapse of a non-spherical body.

2.3 Summary

In this chapter, we have discussed some features of the Kasner metric with a view to then introducing the mixmaster universe. The important point being that in the Kasner metric, one of the directions is contracting and the other two are expanding. We have shown that the mixmaster universe is a cosmology with a singularity which displays very complicated behaviour as we get close to the singularity. We investigated this two ways. First via the analysis by Belinsky, Khalatnikov, Lifschitz analysis and secondly via that done by Misner (who studied a more specific case). Both showed that this particular kind of metric showed similar qualitative behaviour. The metric can be viewed as behaving as a sequence of Kasner metrics in which the contracting directions changes as we pass from one metric to the next. This will allow us to model the mixmaster universe by sticking together a such sequence of Kasner metrics. As our goal is to study spacelike geodesics in this model of the mixmaster universe, we are first of all going to study geodesics in the Kasner metric. Again, doing this will introduce a lot of the notation and equations that we will require when we go on to study the mixmaster universe's geodesics. We will demonstrate that in the Kasner metric, it is possible to get geodesics which bounce arbitrarily close to the singularity. We will return to the mixmaster universe in chapter four.

Chapter 3

Bouncing Geodesics in the Kasner Metric

The aim of this thesis is to study whether or not geodesics can bounce in the mixmaster universe. In order to study geodesics in the mixmaster universe, we are first of all going to look at geodesics in a Kasner metric. Recall that the Kasner metric is given by:

$$ds^2 = -dt^2 + t^{2p_1}dx_1^2 + t^{2p_2}dx_2^2 + t^{2p_3}dx_3^2 \tag{3.1}$$

where the set $\{p_i : i = 1, 2, 3\}$ satisfies the relations:

$$\sum_{i=1}^{3} p_i = \sum_{i=1}^{3} p_i^2 = 1 \tag{3.2}$$

Recall also that this metric has a singularity at $t = 0$. We are interested in whether it is possible for spacelike geodesics heading towards the singularity to turn around before they reach it and so "bounce" away from the singularity. So what are the geodesics for the Kasner metric? Using the Euler Lagrange equations:

$$\frac{d}{ds}\left(\frac{\partial \mathcal{L}}{\partial \dot{x}_i}\right) - \frac{\partial \mathcal{L}}{\partial x_i} = 0 \tag{3.3}$$

where

$$\mathcal{L} = \frac{1}{2}(-\dot{t}^2 + t^{2p_1}\dot{x}_1^2 + t^{2p_2}\dot{x}_2^2 + t^{2p_3}\dot{x}_3^2) \tag{3.4}$$

(so take x_0 to be t) gives us the four geodesic equations of the Kasner metric:

$$\ddot{t} + \sum_{i=1}^{3} p_i t^{2p_i - 1} \dot{x}_i^2 = 0 \tag{3.5}$$

$$t^{2p_i} \dot{x}_i = K_i \tag{3.6}$$

where K_i are constants for $i = 1 \ldots 3$. We want to consider space-like geodesics which have tangent vector $P^a = (\dot{t}, \dot{x}_1, \dot{x}_2, \dot{x}_3)$ satisfying $P^a P_a = 1$. This gives the equation

$$P^a P_a = -\dot{t}^2 + t^{2p_1} \dot{x}_1^2 + t^{2p_2} \dot{x}_2^2 + t^{2p_3} \dot{x}_3^2 = 1$$

and substituting in

$$\dot{x}_i = \frac{K_i}{t^{2p_i}}$$

gives the equation

$$\dot{t}^2 + \left(1 - \sum_{i=1}^{3} \frac{K_i^2}{t^{2p_i}} \right) = 0 \tag{3.7}$$

for spacelike geodesics. We consider this as $\dot{t}^2 + V = 0$ where V is an effective potential given by

$$V(t, p_i, K_i) = 1 - \sum_{i=1}^{3} \frac{K_i^2}{t^{2p_i}} \tag{3.8}$$

In order for a spacelike geodesic to exhibit "bouncing" it must have a time t_b where $\dot{t} = 0$ i.e. when $V(t_b, p_i, K_i) = 0$. From the potential (3.8), one can see that as $t \to 0$ then $V \to -\infty$ and as $t \to \infty$, $V \to -\infty$. Plotting this potential for different values of p_i and K_i shows that this potential increases from $-\infty$ to a maximum then decreases back to $-\infty$. This means that in order for a geodesic with a given set of constants in a given Kasner metric to "bounce", we require that:

$$V_{max} \geq 0 \tag{3.9}$$

So we can consider two equivalent ways of finding out whether or not a given geodesic bounces. We can either look for a solution to $V(t, p_i, K_i) = 0$ or we can find the maximum of the potential and see whether of not it is greater than 0. Both of these methods will require numerical calculations as neither can be done analytically with the potential of the form (3.8), but there are some simplified cases we can look at first.

Suppose we look at a spacelike geodesic in a given Kasner metric which only has one non-zero value of K_i. First, let's consider the case where the non-zero K_i corresponds to the direction with the negative parameter. We are taking this by convention to be p_1 so the geodesic has constants $\{K_1, 0, 0\}$. This geodesic has the potential:

$$V(t) = 1 - \frac{K_1^2}{t^{2p_1}} \tag{3.10}$$

This potential decreases from 1 to $-\infty$. The equation

$$V(t) = 0 \tag{3.11}$$

has the solution

$$t_b = (K_1)^{\frac{1}{p_1}} \tag{3.12}$$

Plotting this potential one can see that this corresponds to a geodesic coming from infinity and bouncing at $t = t_b$. The potential between $t = 0$ and $t = t_b$ is positive which contradicts the geodesic equation (3.7) so this geodesic doesn't exist in that region. The larger the value of K_1 the smaller the value of t_b (as $p_1 < 0$) and hence the closer to the singularity the geodesic bounces. So we can have what we are going to call "purely K_1" geodesics bouncing as close to the singularity as we like. The larger we make K_1 the closer they bounce.

Now let's suppose that instead our geodesic has one of its other constants non-zero. Suppose it has a non-zero K_2 and so has potential:

$$V(t) = 1 - \frac{K_2^2}{t^{2p_2}} \tag{3.13}$$

This time, plotting the potential shows that it increases from $-\infty$ and asymptotes to 1 as t goes to ∞. This means again that there must be a solution to the equation $V = 0$ which is similar to the K_1-case. It is solved by:

$$t_b = (K_2)^{\frac{1}{p_2}} \tag{3.14}$$

but this time only the potential between 0 and t_b can correspond to the geodesic as we must still have $V < 0$ in the geodesic equation. This is the potential of a geodesic which comes out of the singularity then falls back in. (We can see this

through the geodesic equation for $\ddot{t}$, in these geodesics $\ddot{t}$ will always be negative). This time the "bounce" occurs closer to the singularity the smaller the value of K_2 which also makes sense intuitively speaking. In fact this interpretation extends to any geodesic which has $K_1 = 0$ (i.e. one that has both K_2 and K_3 non-zero) as this potential exhibits the same behaviour as the pure K_2 case. The whole plane $K_1 = 0$ only corresponds to geodesics which come out of the singularity then fall back in.

For the spacelike geodesics which have more than one of the K_i non-zero then we are going to have to use numerical calculations to determine whether or not they bounce. But first we are going to see if we can get any intuition about what to expect by investigating what happens to the potential when we start making other constants in pure K_1, K_2, or K_3 geodesics non-zero. It is easiest to demonstrate this by choosing a specific example of a Kasner metric.

3.1 A Specific Example

As an example, let's choose the parameters in the Kasner metric to be:

$$\begin{aligned} p_1 &= \frac{-2}{7} \\ p_2 &= \frac{3}{7} \\ p_3 &= \frac{6}{7} \end{aligned} \tag{3.15}$$

(This corresponds to taking the parameter u to be 2.) First we will plot the potential for some geodesics which are purely K_2 so these have the potential:

$$V(t) = 1 - \frac{K_2^2}{t^{\frac{6}{7}}} \tag{3.16}$$

The potential with $K_2 = 1$ the only non zero constant is plotted in fig (3.1).

We have already shown that if we add in a K_3 term to this potential it doesn't change the overall behaviour of the potential. But what happens if we add in a K_1? This is shown in figure (3.2) with plots of the potentials with $K_2 = 1$ and $K_1 = 0.01$, 0.02, 0.03, 0.04, 0.05.

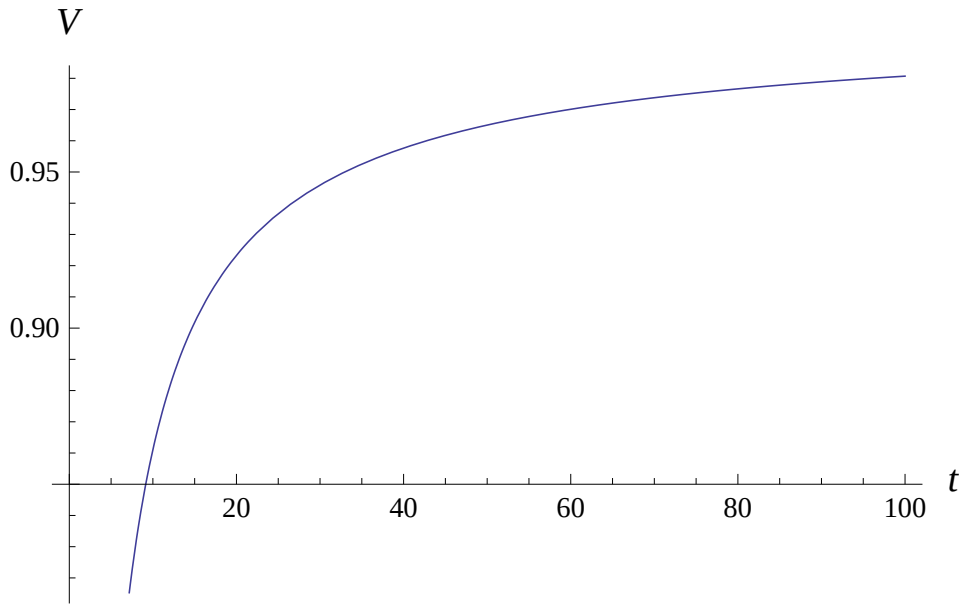

Figure 3.1: A plot of the potential of a geodesic in a Kasner metric ($u = 2$) with $K_2 = 1$, $K_1 = K_3 = 0$.

From this plot we can see that if a small K_1 term is added to this potential, it only affects the potential for large values of t. Its effect is to cause the potential which asymptotes to 1, to "bend around" and fall off back to $-\infty$. This means that the potential will recross the $V = 0$ axis and the part of the potential beyond this point will correspond to a bouncing geodesic of the kind we desire. So a pure K_2 potential with a bit of K_1 added will give us a bouncing geodesic which bounces comparatively far from the singularity (as the K_1 doesn't come into effect until larger values of t are reached). We can also see from figure 3.2 that as we increase the amount of K_1 added, the bounce gets closer to the singularity. However, we can also see that at the same time, the whole potential is lowering so that when K_1 gets large enough, the whole potential will drop below the t-axis and hence the geodesic for that potential will no longer bounce. In this example, this happens around $K_1 \approx 0.58$. For larger values of K_2, the bouncing ceases for smaller values of added K_1 some of which are shown in table 3.1.

Now suppose we start with a potential which is purely K_1. Then we have a geodesic which bounces as close to the singularity as we like. But what happens if

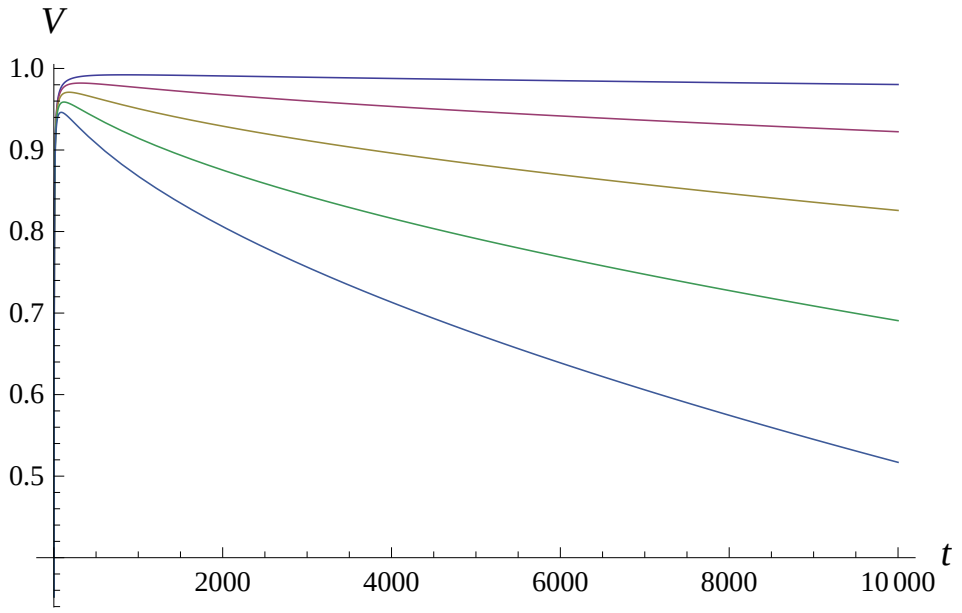

Figure 3.2: A plot of the potentials of a geodesic in a Kasner metric ($u = 2$) with $K_2 = 1$, $K_3 = 0$ and small values of K_1 ranging from 0.01 to 0.05.

K_2	1	2	3	4	5
K_1	0.58	0.36	0.28	0.23	0.20

Table 3.1: A table showing the smallest values of K_1 at which the potential with K_2 stops bouncing.

we add some of another constant into this potential? Let's consider the geodesic with $K_1 = 1$, and $K_2 = K_3 = 0$. This potential bounces at $t = 1$ and is plotted in figure 3.3:

So now we add in a small K_2 term. Plotting the potential in figure 3.4 with $K_1 = 1$ and $K_2 = 0.01, 0.02, 0.03, 0.04, 0.05$ shows that the K_2 affects the potential near $t = 0$ and bends down this side of the potential to $-\infty$.

Zooming in (figure 3.5) around the point where the pure K_1 geodesic bounces ($t = 1$), we can see that adding in a small amount of K_2 slightly shifts the bouncing time of the geodesic towards the singularity. Again, however, as we increase the size of K_2, it lowers the whole potential so that eventually, the whole potential will lie below the t-axis and the geodesic won't bounce. In this specific example this occurs when $K_2 \approx 0.44$.

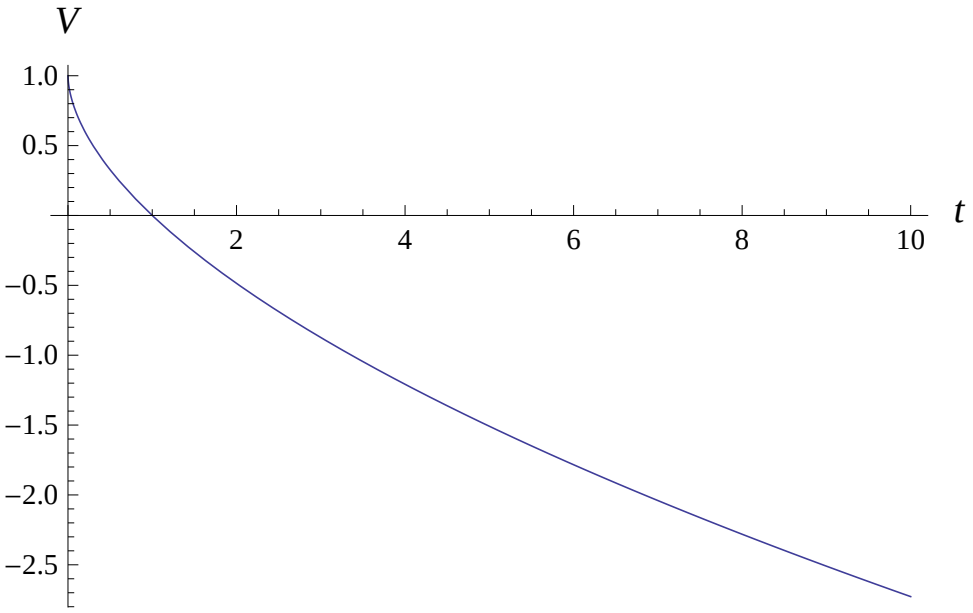

Figure 3.3: A plot of the potential of a geodesic in a Kasner metric ($u = 2$) with $K_1 = 1$, $K_2 = K_3 = 0$.

K_1	1	2	3	4	5
K_2	0.44	0.15	0.085	0.055	0.04

Table 3.2: A table showing the smallest values of K_2 at which the potential with K_1 stops bouncing.

Further investigating shows that the larger we take K_1, then the bouncing ceases at smaller and smaller values of K_2. Some other values are shown in table 3.2 below. Adding in a K_3 term shows similar behaviour but with different numerical values due to the different power of t in the potential.

We are seeking to discover the full region of K_i-space where the bouncing geodesics are found. To summarize the results so far we have:

- All geodesics on the K_1 axis (except the origin), correspond to bouncing geodesics. The further along the axis we go, the closer to the singularity the geodesic bounces.
- The geodesics on the $K_1 = 0$ plane bounce but don't come from infinity.

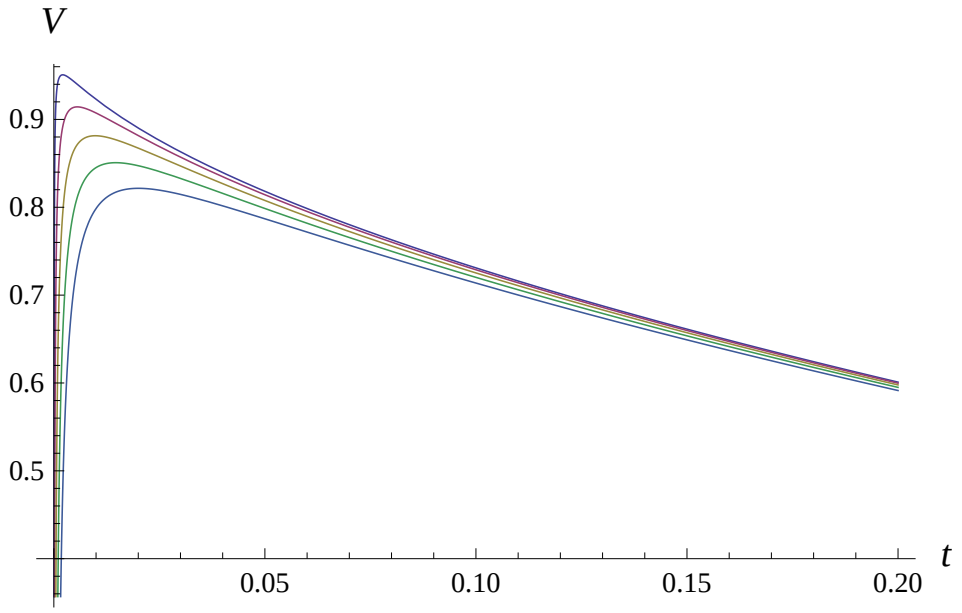

Figure 3.4: A plot of the potentials of a geodesic in a Kasner metric ($u = 2$) with $K_1 = 1$, $K_3 = 0$ and small values of K_2 ranging from 0.01 to 0.05.

- If we move a small distance from the K_1 axis, the corresponding geodesic continues to bounce closer to the singularity but only for a short distance away from the axis.

- If we move a small distance from the other axes, the corresponding geodesic bounces, initially far from the singularity but the bounce gets closer as we move further from the $\{K_1$-$K_2\}$-plane. Again, however this only lasts a short distance until the geodesic stops bouncing.

This gives us a naïve sketch of what region of K-space gives us bouncing geodesics. It will be a sort of funnel shape around the K_1 axis sketched in figure 3.6.

3.2 Numerical Results

We are going to try and plot this region more accurately by numerically calculating which geodesics in K-space bounce. The maximum of the potential of a geodesic can be found numerically in Mathematica, and the region where the maximum is positive, which corresponds to a bouncing geodesic, can be plotted in K_i-space. This was done for a number of values of u and the plots generated are shown in figure

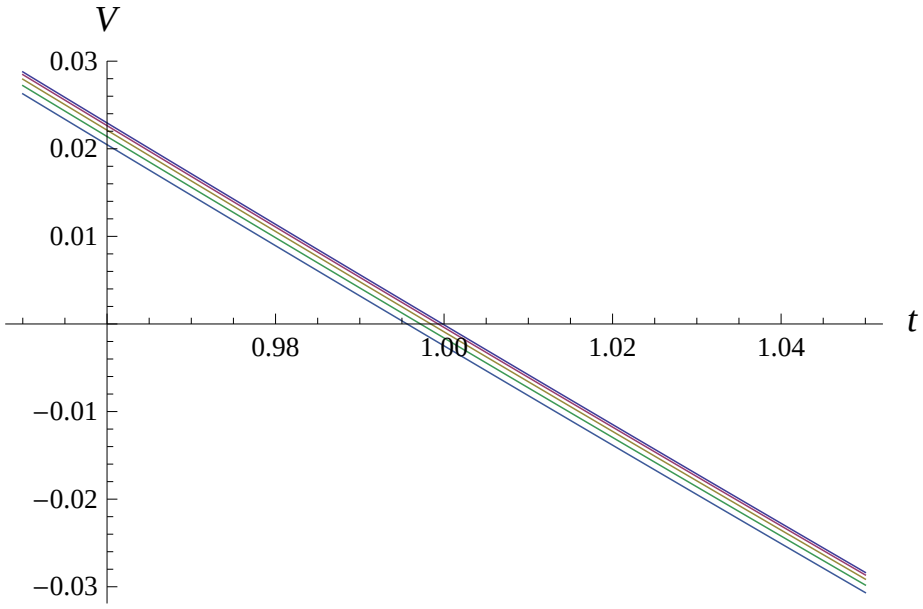

Figure 3.5: A plot of the potentials of a geodesic in a Kasner metric ($u = 2$) with $K_1 = 1$, $K_3 = 0$ and small values of K_2 ranging from 0.01 to 0.05 plotted near the bounce time.

3.7. The values of u chosen were (a)$u = 2$, (b)$u = 3$, (c)$u = 10$, (d)$u = 15$. We can see that the general shape of the bouncing region in K_i-space is what we expected from our analysis above.

In order to understand how the amount of bouncing geodesics varies with u, we would like some way to measure the volume of this region. Presently, as all the constants can range from $-\infty$ to ∞, the volume will always be infinite. In order to get a finite volume we are going to compactify the constants K_i.

3.2.1 Compactifying the Constants

We are going to have compactify the geodesic's constants. There are two reasons for doing this. As they stand each constant can range from negative infinity to infinity. However, as all the constants appear as squared terms in the geodesic equations, we actually only need to consider them between 0 and ∞. But this is still an infinite range giving us an infinite volume of bouncing geodesics. We would like to compactify them so that we can test values of compactified constants in a finite range, corresponding to actual values between 0 and ∞. Then we will have a

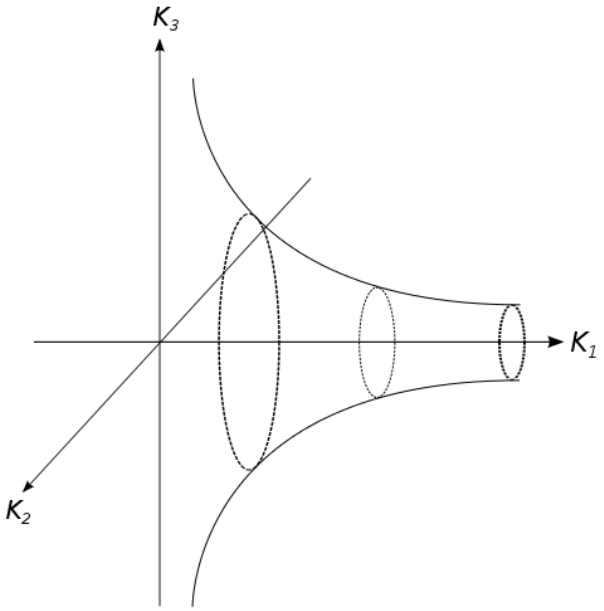

Figure 3.6: A sketch of the region of K_i-space which will give bouncing geodesics in a Kasner metric.

finite space corresponding to bouncing geodesics and so we can measure the volume of this region and see how it changes as we vary the parameter u. There are many functions we can use to do this. The most obvious on to use is:

$$K_i = \tan(k_i) \tag{3.17}$$

where $0 \leq k_i \leq \frac{\pi}{2}$. But there is also a whole family of compactification functions we could use, namely

$$K_i = \frac{-k_i}{k_i^{2n} - 1} \tag{3.18}$$

where n is any natural number and here $0 \leq k_i \leq 1$. Some of these are shown for various values of n in figure 3.8. These were found to be more suitable for the numerical calculations and generally the compactification (3.18) with $n = 1$ was used as for larger values of n, the larger K_i are compactified into a smaller region. As the geodesics which bounce closest to the singularity seem to mostly be found in the regions where K_1 is large, we want these regions to be larger so we can look at the differences here as these are the geodesics we are likely to be most interested in.

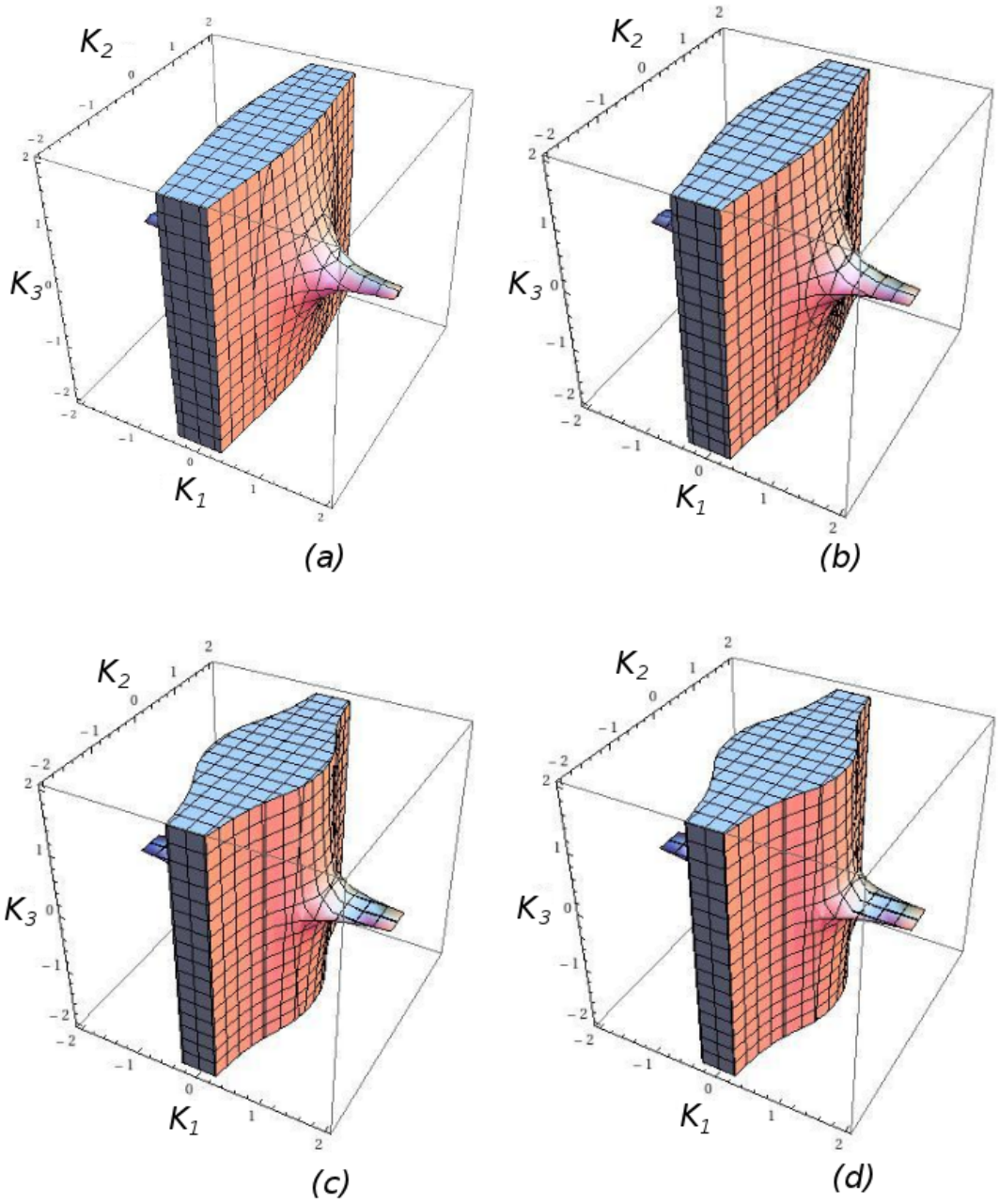

Figure 3.7: Plots of the region of K_i space for geodesics corresponding to bouncing geodesics in a Kasner metric with parameter u where (a)$u = 2$, (b)$u = 3$, (c)$u = 10$, (d)$u = 15$.

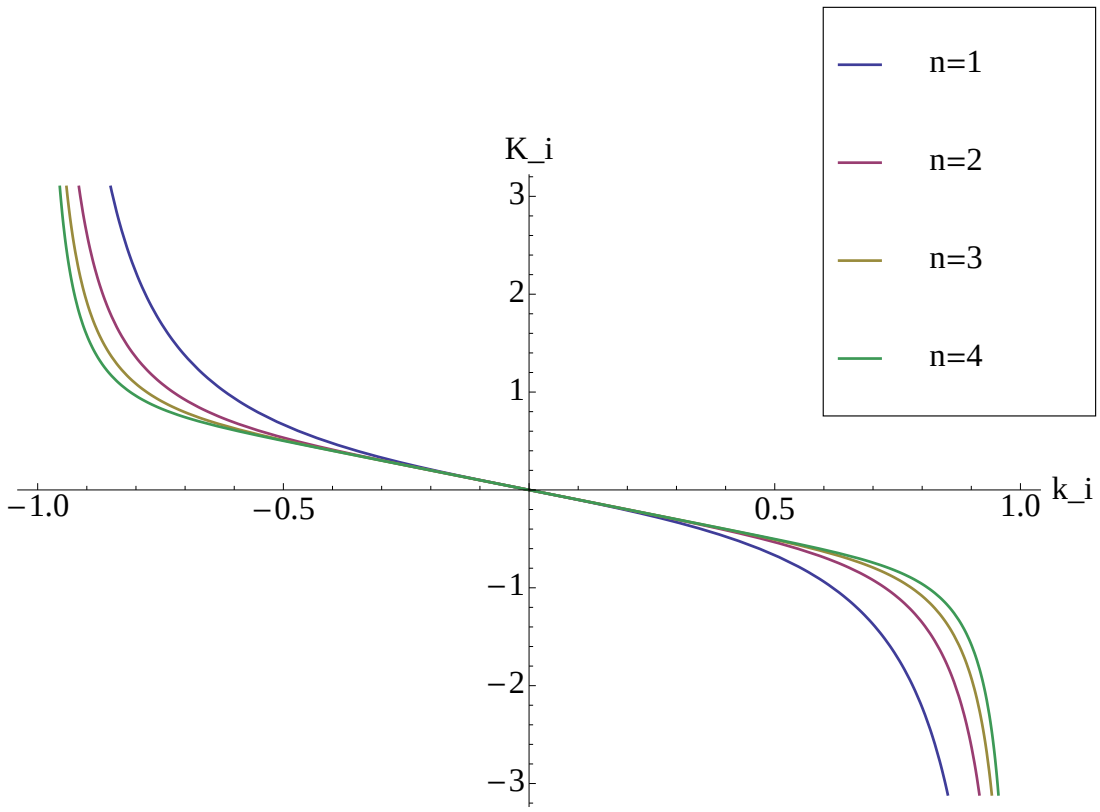

Figure 3.8: A plot of various compactification functions of the form $K_i = \frac{-k_i}{k_i^{2n}-1}$ for the geodesics' constants with different values of n.

3.2.2 Volume of Bouncing Geodesics in Kasner Universe Varying u

We are going to use the compactification of the constants K_i to measure and compare the volume of bouncing geodesics as we vary the parameter u in the metric. To estimate the volume we are going to use a lattice of points in the k_i-space which is now the unit cube. Whether or not these test geodesics bounce will be determined numerically and the number of those that do can be counted to obtain an estimate of the volume of the region of bouncing geodesics.

We are going to look at 1000 points k_1-space. Because taking any of the constants to be either zero or one causes problems with the numerical calculation of the maximum of the potential, we are going to allow the constants to range between

0.01 and 0.91, with an interval of 0.1 between them. We are also going to take the compactification function described in the previous section (3.18) where $n = 1$. The geodesics which bounced were found by numerically calculating the maximum of the potential and testing whether or not it was great than zero. This was done for a range of values u between 1 and 55. Those geodesics which did bounce were counted and the proportion of the total volume of geodesics which bounce against the parameter u is plotted in figure 3.9. This plot shows that the proportion of geodesics which bounce doesn't appear to change very much with the parameter u and always seems to be around about half of the geodesics bouncing.

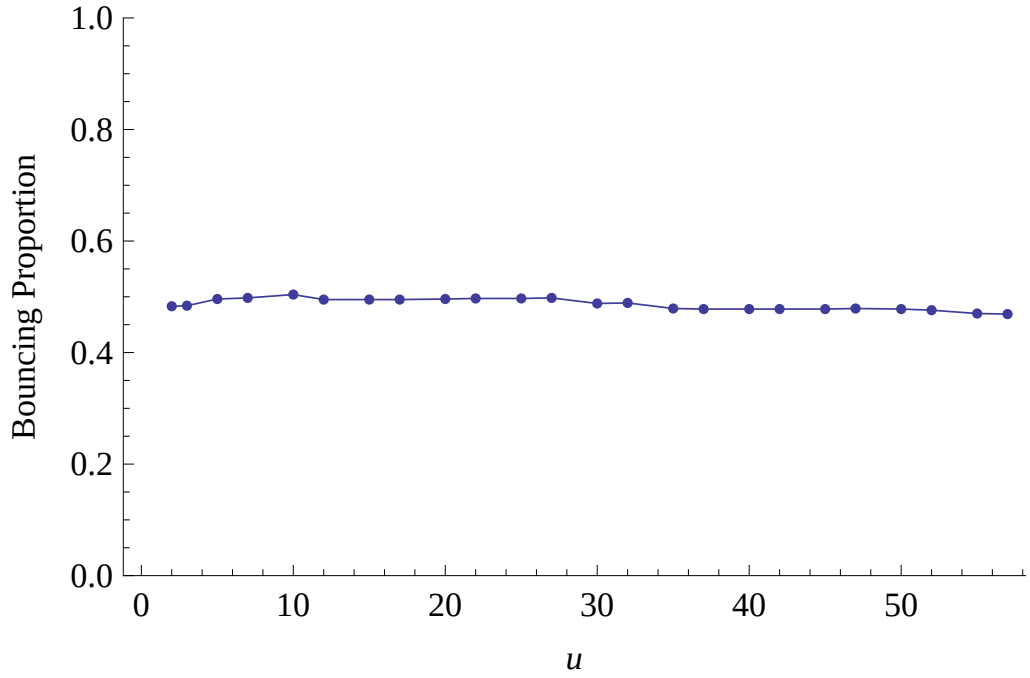

Figure 3.9: A plot of the proportion of k_i-space corresponding to bouncing geodesics for varying u.

This analysis was then repeated varying the parameter n in the compactification. It seemed that as the value of n was increased in the compactification function, the small differences in the proportion of bouncing geodesics are reduced even further because these compactifications suppress large values of the constants so we lose a lot of the bouncing geodesics this way. This is why we have taken the $n = 1$ compactification from now on.

It also may have been possible to amplify the differences in the proportion of bouncing geodesics for varying u by using a finer lattice of test points. Unfortunately, when this was attempted, it was found it made the numerical calculations prohibitively long this making it extremely time consuming to test a large range of values of u.

3.3 Spacelike Geodesics Which Are Nearly Null

We have found a way to measure the proportion of geodesics in K_i-space which bounce, and we have found that we have geodesics which can bounce as close to the singularity as we like along the K_1-axis. We are now interested in how close to null these geodesics are. In order to determine this we are going to have to calculate the proper length of the geodesics. Recall the geodesics were given by the equation:

$$\dot{t}^2 + V(t, K_i, p_i) = 0 \tag{3.19}$$

where $V(t, K_i, p_i)$ is the potential we have been investigating. In other words:

$$\left(\frac{dt}{d\tau}\right) = \sqrt{-V(t, K_i)} \tag{3.20}$$

where τ is proper time along the geodesic. So the path length is given by:

$$\int d\tau = \int \frac{dt}{\sqrt{-V(t, K_i)}} \tag{3.21}$$

For the geodesics to be near null, we want this integral to be as small as possible, so that the proper length of the geodesic is close to zero. Unfortunately, the form of the potential makes this integral impossible to do analytically. We are going to have to use numerical calculations again to work out the integral for all sets K_i. First however, we can look at one simpler situation. Suppose we consider the geodesics which only have K_1 non zero. We have shown these all bounce and can bounce as close to the singularity as we like. So which of this set can we consider to be nearly null? Here the integral (3.21) simplifies considerably and we have the proper length given by:

$$\int \frac{dt}{\sqrt{K_1^2 t^{-2p_1} - 1}} \tag{3.22}$$

Suppose we want to find the path length of the geodesic far away from the singularity i.e. at large t. Then for large t, because the parameter p_1 is negative, the $K_1^2 t^{-2p_1}$ term is much larger than 1. So the above integral is approximately:

$$\begin{aligned} &\sim \int \frac{dt}{\sqrt{K_1^2 t^{-2p_1}}} \\ &= \frac{1}{K_1} \int \frac{dt}{\sqrt{t^{-2p_1}}} \end{aligned} \tag{3.23}$$

So it seems that the path length goes like $\frac{1}{K_1}$ and so would be shorter for larger values of K_1. This implies that the larger the value of K_1, the closer to being null our geodesics are.

When we look at the full K_i-space, we are going to have to use numerical integration to calculate the path length. We numerically integrate the integral (3.21) using Mathematica at a large time and plot the points in k_i-space (so we have compactified the constants again using our usual compactification), colouring the points according to their relative path length (figure 3.10). So in figure 3.10, the points coloured towards the blue end of the spectrum have shorter path length and are closer to null geodesics than those coloured towards the red end (where the black points are the closest to being null of all). From this picture we can see that it is the size of k_1 which has the biggest effect on how close to null the geodesics are, where larger values of k_1 are closer to null than smaller ones. Although increasing the size of the other two constants also makes the geodesics more null, this has a much smaller effect and we need to increase these constants substantially more to get an equivalent reduction in path length.

3.4 Summary

We have shown that in a Kasner metric, you can have spacelike geodesics which bounce as close to the singularity as you like. Moreover, this behaviour is dominated by the size of the constant K_1 in the potential of the geodesic which corresponds to the direction in the metric which is contracting (when looking forwards in time away from the singularity). We then found the full region of bouncing geodesics

and using a compactification for the constants of the geodesics, we showed that the volume of this region does not change much with the parameter u. This means that, in some sense, the "amount" of bouncing in a Kasner metric is not very sensitive to the values of the constants in the metric.

We have also shown that the larger the value of K_1, the smaller the path length of the geodesic and hence these geodesics are the ones that are closer to being null. So it seems that the more null-like a bouncing geodesic is, the closer it bounces to the singularity. The behaviour of geodesics in the Kasner metric is most concisely summarised in the sketch in figure 3.11.

So now we can ask the question as to whether we can get something similar happening in the mixmaster universe introduced in chapter 2, which can be viewed as a sequence of Kasner-like metrics. Can we get spacelike geodesics that bounce close to the singularity?

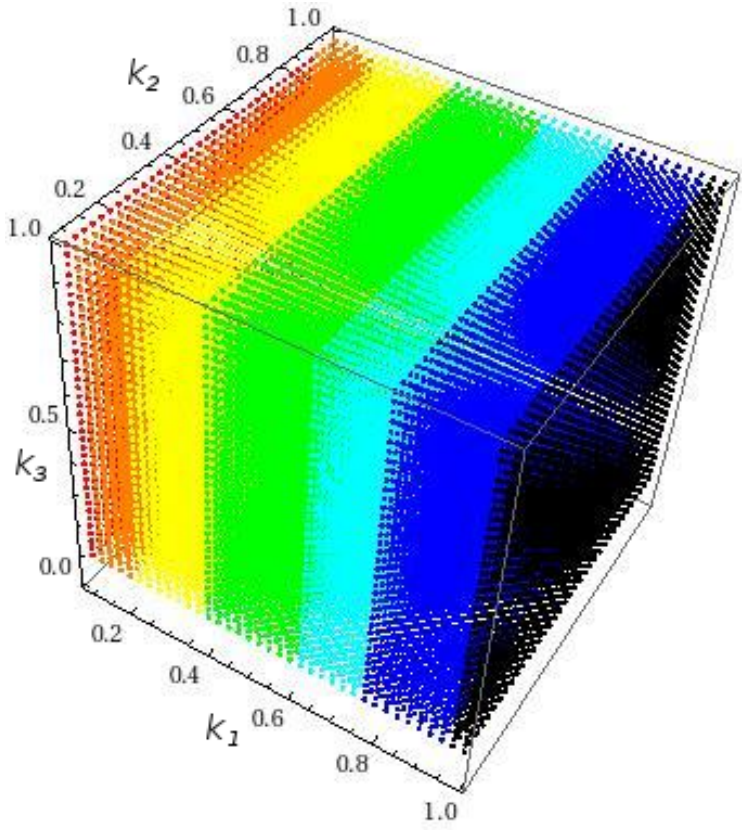

Figure 3.10: A plot of k_i-space with each point coloured by the relative path length of the corresponding geodesic. Those with the shortest path lengths are coloured black and those with longest are coloured red.

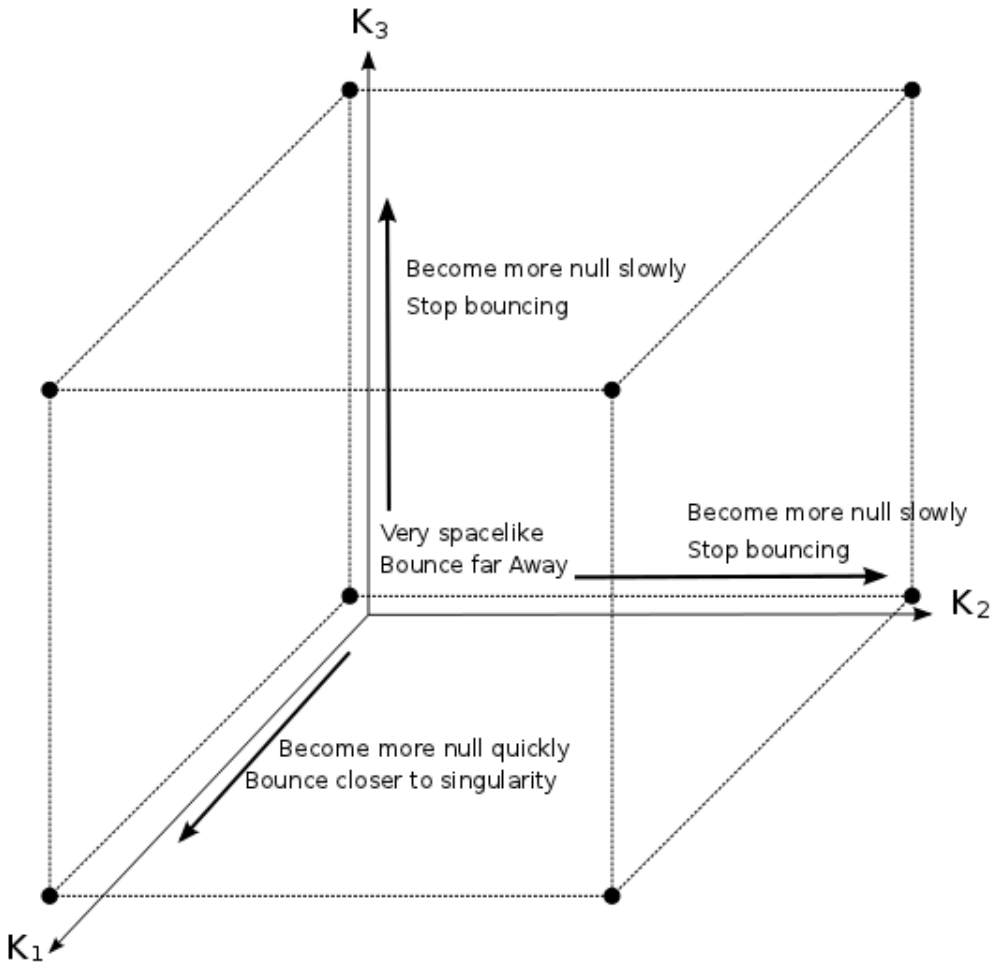

Figure 3.11: A sketch summarising the behaviour of geodesics in a Kasner metric with respect to bouncing and "nullness".

Chapter 4

Geodesics in the Mixmaster Universe

4.1 Modelling the Mixmaster Universe

As introduced in chapter 2, the mixmaster universe evolves as a series of Kasner-like metrics which condense near to the singularity so we are going to construct a model of the mixmaster universe by matching together a sequence of Kasner metrics at transitions times t_i as shown in figure 4.1. We know that in the mixmaster universe, a Kasner metric with parameter u evolves to a Kasner metric with parameter $u-1$ with the appropriate rearrangement of axes (2.14). We are still interested in the spacelike geodesics in this model. A spacelike geodesic in one of these epochs is going to match up to another spacelike geodesic in the next epoch. As discussed, the mixmaster universe has an infinite number of such epochs but we are going to start by considering a finite number of epochs N and try and get an understanding of what happens as N increases.

We are going to look at whether or not, it is possible for geodesics to demonstrate the same kind of bouncing as they did in the pure Kasner universe in this model of the mixmaster universe as illustrated in figure 4.2. First we are going to have to investigate the form of the potential of the spacelike geodesics in the mixmaster universe and derive a condition on these geodesics bouncing as was done for the

spacelike geodesics in a purely Kasner metric.

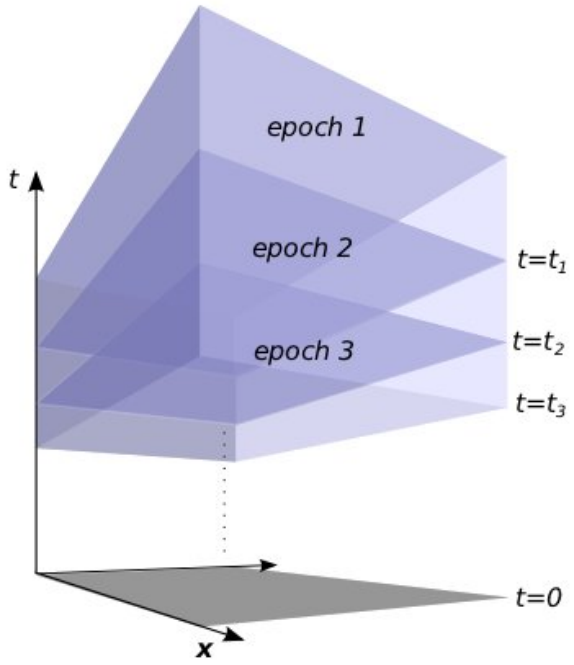

Figure 4.1: An illustration of the model of the mixmaster universe made by matching together a set of Kasner metrics at transition times t_i.

4.1.1 Matching Up the Geodesic Constants

As we are modelling the mixmaster universe by pasting together a series of Kasner metrics, the spacelike geodesics in this model are going to be made by sticking together pieces of spacelike geodesics from each Kasner metric. So in our initial Kasner metric, we will have spacelike geodesics labelled by their constants $\{K_i\}$ and as we cross the transition, the geodesic will become a geodesic in the next Kasner metric with constants $\{\tilde{K}_i\}$. We would like to know how these constants are related. We do this by requiring that at the transition between two epochs, the proper distance between two points remains the same. If we have a transition from one Kasner epoch (with parameters p_i and to another with parameters $\tilde{p}_i$ at time

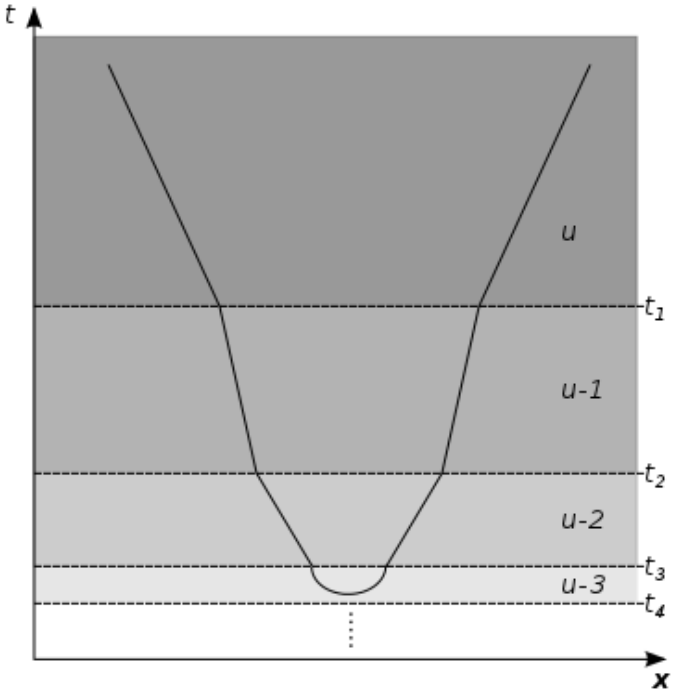

Figure 4.2: A picture of a bouncing geodesic in the mixmaster Universe

$t = t_0$, then the coordinates in the second metric are related to the coordinates in the first via the relation:

$$\tilde{x}_i = t_0^{p_i - \tilde{p}_i} x_i \tag{4.1}$$

Now by (3.6), the constants K_i at $t = t_0$ are given by:

$$K_i = t_0^{2p_i} \dot{x}_i|_{t=t_0} \tag{4.2}$$

and the constants in the second metric are given by:

$$\tilde{K}_i = t_0^{2\tilde{p}_i} \dot{\tilde{x}}_i|_{t=t_0} \tag{4.3}$$

Using these and the above rescaling for $\dot{\tilde{x}}_i$ gives us that:

$$\tilde{K}_i = t_0^{(\tilde{p}_i - p_i)} K_i \tag{4.4}$$

So a geodesic with constant set $\{K_i\}$ will become the geodesic with constants $\{\tilde{K}_i\}$ as it crosses the transition into the next Kasner epoch. This geodesic will have the geodesic equation:

$$\dot{t}^2 + V = 0 \tag{4.5}$$

where V is a piecewise potential made up of the potentials corresponding to the constants of the geodesic in each Kasner epoch. Again we want this geodesic to come from infinity (so the potential has to be negative for suitably large time t) which means that it cannot be purely K_2 or K_3 in the first epoch. And for the geodesic to bounce, we again require that there is at least one point at which the now piecewise potential V is zero. Essentially what we are looking for are geodesics which match up in such a way that they reach an epoch where their constants are such that, in that Kasner metric, they bounce in the right time period.

We would like to investigate further how the K_i evolve through the Kasner epochs as similarly to the pure Kasner case, once we have found geodesics which bounce, we would like to determine how close to being null, these bouncing geodesics are. We can see from the relations (4.4) above that the evolution of the K_i depends upon both the transition time and the constants p_i, $\tilde{p}_i$ in the Kasner metrics involved. The relation above tells us that each time a geodesic crosses a transition t_i, its constants get multiplied by a factor

$$t_0^{(\tilde{p}_i - p_i)} \tag{4.6}$$

If we write the p_i in terms of the parameter u, and take p_1 to be negative and such that $u > 1$. Then we have:

$$\begin{aligned} p_1(u) &= \frac{-u}{1+u+u^2} \\ p_2(u) &= \frac{u+1}{1+u+u^2} \\ p_3(u) &= \frac{u(u+1)}{1+u+u^2} \end{aligned} \tag{4.7}$$

then this means that the $\tilde{p}_i$ become (via the evolution rule of these parameters):

$$\begin{aligned} \tilde{p}_1 &= \frac{u}{1-u+u^2} \\ \tilde{p}_2 &= \frac{1-u}{1-u+u^2} \\ \tilde{p}_1 &= \frac{u(u-1)}{1-u+u^2} \end{aligned} \tag{4.8}$$

So in terms of t_0 and u, the three exponents in the multiplication factors for the K_i

are:

$$\begin{aligned} \tilde{p}_1 - p_1 &= \frac{2(u+u^3)}{1+u^2+u^4} \\ \tilde{p}_2 - p_2 &= \frac{-2u^3}{1+u+u^4} \\ \tilde{p}_3 - p_3 &= \frac{-2u}{1+u+u^4} \end{aligned} \tag{4.9}$$

As we have prescribed u to be larger than 1, this means that two of these exponents are negative and the other is positive. If $t_0 < 1$ this means that two of the constants will get larger and the other will get smaller. The opposite would be true for $t_0 > 1$ but we are generally going to be taking our first transition to occur at $t_0 = 1$ as explained in the next section so the rest of the transitions will occur at $t < 1$.

Observing this evolution over time, showed that the size of the constants for a given geodesic could fluctuate by quite large amounts. So while we could start off with a geodesic with say a very large value of K_1 compared with the other constants, this constant can fluctuate between being very large and very small as it evolves through the Kasner epochs. This means looking back to the picture we had (figure 3.10), it is not clear which geodesics can be considered nearly null. We can think about the constants evolving and moving around this picture, and so how close to being null they are can change quite drastically as the epochs evolve depending on how the parameters of the metric evolve. Nevertheless, once we have found bouncing geodesics, it might be possible to say something about how close to null they are either in the first epoch or in subsequent epochs as we now know how their constants evolve through the epochs.

The other ingredient we need in our model of the mixmaster universe is a set of times t_i at which the transitions occur.

4.1.2 Transition Time Schemes

We are considering a model of the mixmaster universe where we have a sequence of Kasner epochs matched together at a set of transition times $\{t_i\}$. We are going to investigate these transition times a little further.

First we are going to demonstrate that, without loss of generality, we can set the first transition to occur at $t = 1$ by rescaling t. Suppose we have two Kasner metrics matched together and the first transition occurs at $t_1 = \alpha$. The geodesics in this model then have the piecewise potential:

$$V(t) = \begin{cases} 1 - \sum_{i=1}^{3} \frac{K_i^2}{t^{2p_i}} & t > \alpha \\ 1 - \sum_{i=1}^{3} \frac{\tilde{K}_i^2}{t^{2\tilde{p}_i}} & t < \alpha \end{cases} \tag{4.10}$$

Then let $t = \alpha\sigma$ and rewrite the piecewise potential in terms of σ. For $t > \alpha$, i.e. $\sigma > 1$

$$\begin{aligned} V = V_1 &= 1 - K_1^2\alpha^{-2p_1}\sigma^{-2p_1} - K_2^2\alpha^{-2p_2}\sigma^{-2p_2} - K_3^2\alpha^{-2p_3}\sigma^{-2p_3} \\ &= 1 - M_1^2\sigma^{-2p_1} - M_2^2\sigma^{-2p_2} - M_3^2\sigma^{-2p_3} \end{aligned} \tag{4.11}$$

where $M_i = \alpha^{-p_i}K_i$.
For $t < \alpha$ i.e. $s < 1$, we have

$$V = V_2 = 1 - \tilde{K}_1^2\alpha^{-2\tilde{p}_1}\sigma^{-2\tilde{p}_1} - \tilde{K}_2^2\alpha^{-2\tilde{p}_2}\sigma^{-2\tilde{p}_2} - \tilde{K}_3^2\alpha^{-2\tilde{p}_3}\sigma^{-2\tilde{p}_3} \tag{4.12}$$

Now $\tilde{K}_i = K_i\alpha^{\tilde{p}_i - p_i}$. So substituting this into the equation above we get

$$\begin{aligned} V_2 &= 1 - K_1^2\alpha^{-2p_1}\sigma^{-2\tilde{p}_1} - K_2^2\alpha^{-2p_2}\sigma^{-2\tilde{p}_2} - K_3^2\alpha^{-2p_3}\sigma^{-2\tilde{p}_3} \\ &= 1 - M_1^2\sigma^{-2\tilde{p}_1} - M_2^2\sigma^{-2\tilde{p}_2} - M_3^2\sigma^{-2\tilde{p}_3} \end{aligned} \tag{4.13}$$

We can see that this is the same as a potential (3.8) where the transition occurs at $t = 1$ with a rescaled set of constants. If we have more than two epochs in the model then the other bits of the potential will also be similarly rescaled and so from now on we will generally assume that $t_1 = 1$ (i.e. the first transition). There may be some cases later, however where it is useful to assume that the first transition occurs at different, larger times.

4.2 Bouncing Geodesics in a "Regular" Time Transition Scheme

We would now like to find the bouncing geodesics in a mixmaster universe, according to the model we set up in the previous section. This will be done in a similar way to the calculations for the pure Kasner metric but there will be some complications.

The model for the Mixmaster Universe requires several parameters. It requires an initial u from which the expansion and contraction parameters in all the subsequent Kasner epochs are determined and it also requires a set of transition times. In this chapter, we will only consider the simplest set of transition times. We want the epochs to condense and get closer and closer together as we get towards the singularity so we will take our set of transition times to be of the form $t_i = \frac{1}{m^{i-1}}$, where m is a natural number, so this is some geometric series. Note that if we reconsider the potential in terms of $\log t$ these would become regularly spaced transition times and for this reason we shall refer to them as "regular" transition time schemes.

In order to gain insight into what happens for infinitely many epochs, we are going to consider a set of N Kasner epochs matched together as in the previous chapter and observe what happens to the region of bouncing geodesics as N increases. The full mixmaster universe would have an infinite number of such epochs so we want to know what happens as $N \to \infty$.

This means each geodesic, with an initial set of compactified constants k_i, will have a potential made up of N pieces of various Kasner geodesics' potentials. All we need to do to see if any given geodesic bounces is to determine whether or not its potential is ever positive. Due to the complexity of the potential's equations, we are going to have to do this numerically. As in the Kasner case, there are two ways we can approach it. We can either try to solve the equation $V = 0$ numerically and directly find the time at which the geodesic bounces or as we did for the Kasner universe, we can numerically find the global maximum of the potential. If it is positive

then we know the geodesic bounces. But now the piecewise nature of the potential causes a some trouble.

One difficulty in finding the roots of the potential is that they can occur at any time between 0 and ∞. Also, whereas in the pure Kasner case there are only ever a maximum of two roots, if we increase the number of Kasner epochs then it is possible for the potential to have more than one root. At some level, this is not an issue if one is only interested in whether or not geodesics bounce, as only the geodesics with no roots don't bounce. However, it does cause problems when we are trying to determine in which epoch the bouncing has occurred. The geodesic we are interested in bounce at the largest root and it can be difficult to be sure that the largest root has been found when evaluating them numerically.

We have a similar problem when trying to determine the maximum of the potential. In the pure Kasner case, there could only ever be one global maximum but as we match together potentials we can have potentials that have more than one local maximum. Again it can be difficult to ensure that the maximum found numerically is the global maximum when we are dealing with an infinite range of times.

These problems can be dealt with in a similar way as was done for the constants k_i, by introducing a compactification of the time so that we can search for either the global maximum, or the roots of the potential in a finite range only. We are going to take

$$t = \tan(s) \tag{4.14}$$

where $s \in [0, \frac{\pi}{2})$. So now we only need to seek roots or global maxima in a finite region. However, due to the slow speed at which Mathematica calculates maxima of piecewise functions, it was found to be more efficient to mount a two-stage attack. First, the value of the potential at 10 regularly spaced test times is evaluated. If any of these is positive then we know that at some stage prior to that time (i.e. at a larger value of t), the geodesic has bounced. This means that many of the bouncing geodesics are found very quickly. Then, only if this condition fails and all these test

points along the potential are negative, is the global maximum found numerically (which takes longer).

4.3 Numerical Results

To determine the proportion of the geodesics which bounce, we use 1000 test points in k_i-space (where again we are compactifying the constants using (3.18) with $n = 1$) and see how the number of those that bounce changes as we increase N, the number of Kasner epochs. So when there is only one epoch we have a Kasner metric as discussed in the previous chapter. We then splice in more epochs according to the rules for the evolution of the metric. So each time we add an epoch, the potential for each geodesic gains another piecewise component. We are going to take the first transition to occur at $t = 1$ and use the transition time scheme

$$t_i = \frac{1}{m^{i-1}} \tag{4.15}$$

with $m = 2$.

This was done for many initial values of u and similar behaviour was observed for all cases, an example of which is shown in figure 4.3 where $u = \sqrt{7}$. It was also repeated for different transition time schemes with different values of m. Again, these showed very similar behaviour to that seen in figure 4.3. When $N = 1$, we have the pure Kasner metric case which we have already studied. For two Kasner epochs, the proportion of bouncing geodesics drops significantly. This is because splicing in the second epoch would "cut off" the tail of the bouncing region for the pure Kasner case which were the geodesics which would have bounced after the transition when looking back in time towards the singularity (i.e. those that bounced between $t = 0$ and $t = 1$). Going from 2 to 3 epochs tended to show a slight increase (we will discuss this further later) in the proportion of bouncing geodesics but after that, as N increased, the proportion of bouncing geodesics remained constant. In fact, on closer inspection, it was discovered that for larger values of N, it was always the same set of geodesics that bounced and that they were doing so in the first Kasner epoch and that the same was happening in all the transition schemes of this type

and all the values of u that were tried. The only effect of adding further Kasner epochs at these "regular" transition times was to cut off all those geodesics that would have bounced between $t = 0$ and $t = 1$ in the pure Kasner metric. This led to an analytic proof, that it was impossible for a geodesic that did not bounce in the first Kasner epoch to bounce in any subsequent epoch in a "regular" time transition scheme.

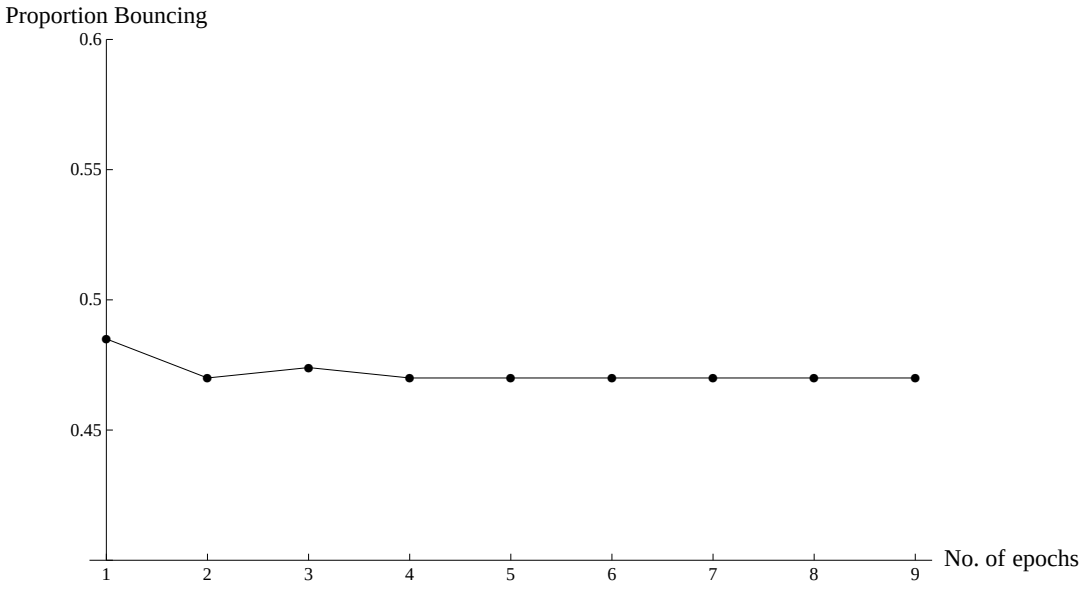

Figure 4.3: A plot of the proportion of k_i space which corresponds to bouncing geodesics for increasing numbers of epochs with initial $u = \sqrt{7}$

4.4 Impossibility of Bouncing After the First Epoch in Regular Time Transitions

We are now going to show analytically that if a geodesic does not bounce in the first epoch, then it will not bounce in the second epoch either. Suppose we just consider two Kasner epochs matched together at a transition time of $t_1 = 1$. Then a geodesic has a potential

$$V(t, u, K_i) = \begin{cases} V_1(t, u, K_i) & t > 1 \\ V_2(t, u, K_i) & t < 1 \end{cases} \tag{4.16}$$

So suppose the geodesic does not bounce in the first epoch. This means the potential must remain below 0 for $t > 1$ i.e..

$$V_1 = 1 - K_1^2 t^{-2p_1(u)} - K_2^2 t^{-2p_2(u)} - K_3^2 t^{-2p_3(u)} < 0 \tag{4.17}$$

or

$$\begin{aligned} K_1^2 t^{-2p_1(u)} &+ K_2^2 t^{-2p_2(u)} + K_3^2 t^{-2p_3(u)} \\ = K_1^2 t^{\left(\frac{2u}{1+u+u^2}\right)} &+ K_2^2 t^{\left(\frac{-2(u+1)}{1+u+u^2}\right)} + K_3^2 t^{\left(\frac{-2u(u+1)}{1+u+u^2}\right)} > 1 \end{aligned} \tag{4.18}$$

Now for $t < 1$,

$$V_2 = 1 - K_1^2 t^{-2p_2(u-1)} - K_2^2 t^{-2p_1(u-1)} - K_3^2 t^{-2p_3(u-1)} \tag{4.19}$$

We want to show that this is always negative for $t < 1$. So consider

$$K_1^2 t^{-2p_2(u-1)} + K_2^2 t^{-2p_1(u-1)} + K_3^2 t^{-2p_3(u-1)} \tag{4.20}$$

Let's rewrite this in terms of $s = \frac{1}{t}$. So we have

$$\begin{aligned} K_1^2 s^{2p_2(u-1)} &+ K_2^2 s^{2p_1(u-1)} + K_3^2 s^{2p_3(u-1)} \\ = K_1^2 s^{\left(\frac{2u}{1-u+u^2}\right)} &+ K_2^2 s^{\left(\frac{-2(u-1)}{1-u+u^2}\right)} + K_3^2 s^{\left(\frac{-2u(1-u)}{1-u+u^2}\right)} \end{aligned} \tag{4.21}$$

where $s > 1$

Now note

$$\begin{aligned} s^{\frac{2u}{1-u+u^2}} &= s^{\frac{2u}{1+u+u^2}} s^{\frac{4u^2}{1+u^2+u^4}} \\ s^{\frac{-2(u-1)}{1-u+u^2}} &= s^{\frac{-2(u+1)}{1+u+u^2}} s^{\frac{4}{1+u^2+u^4}} \\ s^{\frac{-2u(1-u)}{1-u+u^2}} &= s^{\frac{-2u(u+1)}{1+u+u^2}} s^{\frac{4u^4}{1+u^2+u^4}} \end{aligned} \tag{4.22}$$

This means that as $s > 1$, every term in the expression in (4.20) is larger than the equivalent term on the left hand side of the inequality (4.17). Therefore (4.20) is always greater than (4.17) i.e.. larger than 1. So the potential in the second epoch is always negative too and hence the geodesic doesn't bounce.

We have basically shown that across a transition, $V_2(\frac{1}{t}) < V_1(t)$ (i.e. the potential on the side closer to the singularity will always be lower than an equivalent point on

the other side of the transition). This leads to the conclusion that if the transitions occur within a time scheme of the form $\frac{1}{t_0^n}$ for $n = 0, 1, 2, \ldots$, which we have been calling "regular" transitions, then if a geodesic doesn't bounce in the first epoch, it will not bounce in any of the subsequent epochs.

4.5 A Caveat

We noted above that as we increased the number of epochs from 2 to 3, the proportion of bouncing geodesics did show a slight increase. This would seem to be counter to the reasoning above, but on closer inspection of the times at which the bouncing occurs, it can be seen that this is not a problem. The proof in the previous section basically shows that if we have 2 epochs then the geodesics which don't bounce in the first cannot bounce in the second. But when we increase to 3 epochs something a little different happens.

We are going to consider three Kasner epochs and we are going to set the transition times to be at $t = 1$ and $t = t_0$ where $t_0 > 1$. A geodesic has potential V_1 for $t > t_0$ (epoch 1), V_2 for $1 < t < t_0$ (epoch 2) and V_3 for $t < 1$ (epoch 3). Suppose the geodesic doesn't bounce in epoch 1. Then we know the proof above prevents the geodesic from bouncing in epoch 2. Now consider the transition from epoch 2 to epoch 3. The work above tells us that $V_3(\frac{1}{t}) < V_2(t)$ but as we know V_2 is only negative between 1 and t_0, then we can only deduce that V_3 is negative between $\frac{1}{t_0}$ and 1. It is possible for V_3 to be positive between 0 and $\frac{1}{t_0}$. This is what accounts for the slight rise in the numerical results. Some extra geodesics are allowed to bounce by virtue of the third epoch being longer than it should be. When we add another epoch, the geodesics which bounce here are cut off again. This would also cause variations for higher numbers of epochs as whenever we have a finite number of epochs, the last epoch before the singularity is always longer than it should be. While slight variations were seen in the numerical results, it is not clear whether this is the cause as opposed to slight errors. Also, the variations may be so small that the lattice spacing of the test points might not be small enough to catch these

small areas of bouncing geodesics. If we have an infinite number of epochs, however, none of the geodesics can get through in this way and hence all the geodesics which do so, bounce in the first Kasner epoch. This leads to an interesting subsequent question. What if we perturb this scheme of "regular" time transitions? If we make one of the epochs somewhere in the evolution a little longer than it would be in a regular scheme, does this give some geodesics the opportunity to bounce in later epochs. This is the question that is investigated in the next chapter.

4.6 Summary

In this chapter we have set up a model of the mixmaster universe by matching together a sequence of Kasner metrics. We have discussed the ingredients required for this model, namely a scheme of transition times and the form of the potential for a spacelike geodesic as a piecewise potential made up from parts of Kasner spacelike geodesics. We have also discussed how to determine whether or not geodesics bounce away from the singularity in this model.

We have then shown that if we have a logarithmically regular set of time transitions (which we are calling "regular"), then we cannot have any geodesics bouncing after the first Kasner epoch. Numerical results motivated the search for an analytic proof which showed that this was indeed the case. In such a mixmaster universe with these kinds of time transitions, regardless of the starting u, spacelike geodesics either bounce away in the first epoch or fall into the singularity. This means that there is no way to study the singularity using bouncing geodesics. However, we noticed a slight caveat in our argument means there are some geodesics which could bounce if one of the epochs is a little longer. So it appears that if we have a more irregular time transition scheme, then there are some geodesics which could be given the opportunity to bounce beyond the first epoch. This is what we are going to consider in the next chapter.

Chapter 5

Moving Away From "Regular" Time Transitions

We have proven in the previous chapter that if the transition times between Kasner epochs occur within a geometric series, then we cannot have any geodesic bouncing after the first Kasner epoch. This is because the piecewise potential of the geodesic is such that as we go across a transition (towards the singularity), the potential in the new epoch remains below an equivalent point in the previous Kasner epoch. So now we are going to look at what happens when we perturb the transition times around these geometric sequences. This is because it was also observed that if we consider a more irregular time scheme, it might be possible that by making later epochs a little longer than they would be under "regular" transitions, then that could give some geodesics which didn't bounce in the first epoch the chance to bounce in a longer epoch.

5.1 An Example

To show that this is a reasonable way to proceed, we can show some explicit examples where it would be possible for such bouncing to occur. Suppose, as an example, we take a set of three epochs. We are going to take the transitions between these epochs to occur at $t = 2$ and $t = 1$. We are going to take $u = \sqrt{7}$ again. Plotting the potential for various values of k_1, k_2 and k_3, we can find examples such the one

illustrated in figure 5.1. Here we have $k_1 = 0.71$, $k_2 = 0.08$, $k_3 = 0.1$ and we take the transitions to occur at $t = 2$ and $t = 1$.

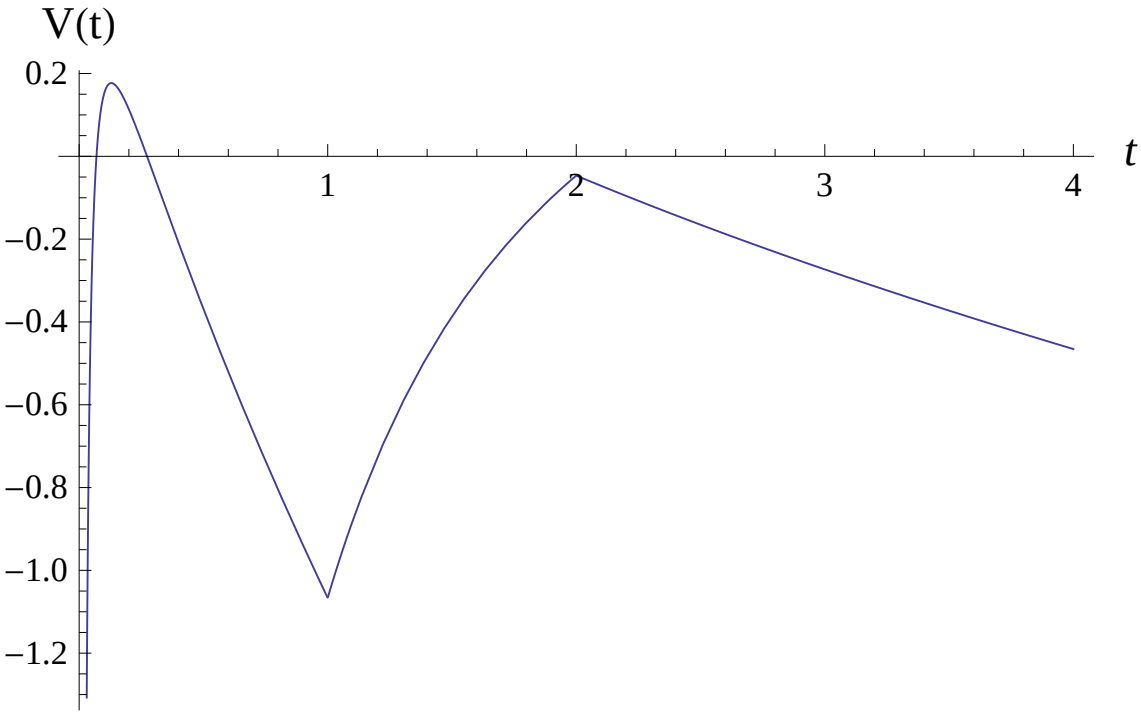

Figure 5.1: A plot of the potential of a geodesic with constants $\{0.71, 0.08, 0.1\}$ in a mixmaster universe with 3 epochs, with initial $u = \sqrt{7}$.

In this plot, we can see that if the next transition were to occur at $t = \frac{1}{2}$ as per the "regular" time scheme, then this would cut off the potential before it reaches zero. However, if we were to delay that transition by a suitable amount then this geodesic, which hasn't bounced in the first epoch, would have the opportunity to bounce. In fact there is a little region of k_i-space around this point where this continues to happen. Roughly it seems that k_1 can be between 0.71 and 0.74, k_2 between 0 and 0.12 and k_3 between 0 and 0.21, that this behaviour still occurs and we can find similar behaviour and similar albeit small regions of bouncing for many other values of u.

We are now going to analytically derive some inequalities that are required for such a region of bouncing to exist.

5.2 Some Inequalities

We have seen via examples that it is indeed possible in a 3 epoch scenario to have geodesics bouncing in the third epoch which did not bounce in the previous two because the third epoch is longer than the previous two and that it seems that there is a small region of k_i space where this is possible. Now we are going to derive some inequalities on the geodesics' constants will have to satisfy in order for this bouncing to occur.

Suppose we have the same set-up as in the previous discussion where we have three epochs, the first transition at $t = t_0 > 1$ and the second at $t = 1$. For ease of notation (namely because the constants don't change as the cross the $t = 1$ transition) we are going to write the potential of a geodesic in terms of its constants in this middle epoch. We will call these constants $\{M_i\}$ in order to distinguish them from the constants $\{K_i\}$ in the first epoch. We also have a set of parameters for each of the Kasner metrics. They are $\{p_1, p_2, p_3\}$, $\{p_1', p_2', p_3'\}$ and $\{p_1'', p_2'', p_3''\}$. So the potential for a geodesic in this set-up is:

$$V(t, u, M_i) = \begin{cases} 1 - \sum t_0^{2(p_i - p_i')} \frac{M_i^2}{t^{2p_i}} = V_1(t) & t > t_0 \\ 1 - \sum \frac{M_i^2}{t^{2p_i'}} = V_2(t) & 1 < t < t_0 \\ 1 - \sum \frac{M_i^2}{t^{2p_i''}} = V_3(t) & t < 1 \end{cases} \tag{5.1}$$

Note that the factor $t_0^{(p_i - p_i')}$ is what rescales the constants M_i to the constants K_i.

We can write all the constants p_i, p_i' and p_i'' in terms of the parameter u. So if we write p_1, p_2 and p_3 as $p_1(u)$, $p_2(u)$, $p_3(u)$ according to (2.14), then the other constants become:

$$\begin{aligned} p_1'(u) &= p_2(u-1) \\ p_2'(u) &= p_1(u-1) \\ p_3'(u) &= p_3(u-1) \end{aligned}$$

and also:

$$\begin{aligned} p_1''(u) &= p_1(u-2) \\ p_2''(u) &= p_2(u-2) \\ p_3''(u) &= p_3(u-2) \end{aligned}$$

Note that we have made no assumption about the size of u and thus do not know which constants are positive and negative beyond the first set where we have chosen $p_1(u)$ to be negative.

5.2.1 Upper Bounds on Two Constants

We are aiming to find conditions on the M_i (and hence on the K_i) for the geodesic to bounce in the third epoch. We assume it has not bounced in the first and therefore know it does not bounce in the second. We also know that if it does bounce it will have to be at a time $t_b < \frac{1}{t_0}$. So let's consider $V_3(t)$ when $t < \frac{1}{t_0}$.

$$V_3(t) = 1 - \frac{M_1^2}{t^{2p_1(u-2)}} - \frac{M_2^2}{t^{2p_2(u-2)}} - \frac{M_3^2}{t^{2p_3(u-2)}} \tag{5.2}$$

For the geodesic to bounce, we require the potential to be positive at some point i.e. that there exists a time $T < \frac{1}{t_0}$ for which $V_3(T) > 0$. This gives that:

$$\frac{M_1^2}{T^{2p_1(u-2)}} + \frac{M_2^2}{T^{2p_2(u-2)}} + \frac{M_3^2}{T^{2p_3(u-2)}} < 1 \tag{5.3}$$

As the sum of the three terms is less than one, and all the terms are squares, this means that each individual term must also be less than one. So we have that there exists a time T such that:

$$\frac{M_1^2}{T^{2p_1(u-2)}} < 1 \tag{5.4}$$

$$\frac{M_2^2}{T^{2p_2(u-2)}} < 1 \tag{5.5}$$

$$\frac{M_3^2}{T^{2p_3(u-2)}} < 1 \tag{5.6}$$

Or more generally:

$$M_i < T^{p_i(u-2)} \tag{5.7}$$

Now we have to worry about the signs of the p_i. As we know that $T < \frac{1}{t_0}$, then these two facts will only give us inequalities for the M_i for those where the corresponding p_i are positive. So if we have $p_1 < 0$ (which means $u > 2$), the inequalities we get are

$$M_2 < \left(\frac{1}{t_0}\right)^{p_2(u-2)} \tag{5.8}$$

$$M_3 < \left(\frac{1}{t_0}\right)^{p_3(u-2)} \tag{5.9}$$

Note that there are two other cases. If $1 < u < 2$ or $u < 1$ then we get similar inequalities for M_1,M_2 or M_1,M_3 respectively. So we have derives some upper bounds on the value of two of the constants M_i in order for the geodesic to bounce at some point in the third epoch.

5.2.2 A Crude Lower Bound

In the previous section we only managed to derive upper bounds for two of the three geodesic constants. We would like a bound on the third. We can introduce a very crude bound quite easily. Recall that we require that the geodesic does not bounce before the third epoch and that this means the potential of the geodesic must be negative for all values of $t > \frac{1}{t_0}$. Specifically, we must have that the potential is negative at $t = 1$. Looking at the potential (5.1), this means that the constants must satisfy the relation:

$$M_1^2 + M_2^2 + M_3^2 > 1 \tag{5.10}$$

So if, for example we have (as above) upper bounds for M_2 and M_3 (i.e. $u > 2$), this relation will give us a lower bound for M_1. Namely that:

$$M_1 > \sqrt{1 - \left(\frac{1}{t_0}\right)^{p_2(u-2)} - \left(\frac{1}{t_0}\right)^{p_3(u-2)}} \tag{5.11}$$

There would be similar relations for M_2 and M_3 for the cases where $u < 2$. We would like to also find an upper bound on this third constant and this can be done by slightly altering the situation we are looking out.

It is important to note at this stage that a geodesic which bounces will satisfy all the conditions found so far but that satisfaction of the inequalities does not guarantee that the corresponding geodesic DOES bounce. It merely introduces the possibility of bouncing to a region of geodesics.

5.3 Epsilon Perturbations in Transition Times

We are going to look at a slightly different situation. Suppose we have a similar set-up as before. We have three Kasner epochs with transitions at t_0, and 1 so the potential is of the form (5.1). But now we are going to require that the next transition happens within ε of the next log regular transition so the third transition will occur at $t = \frac{1}{t_0} - \varepsilon$. We want to find out the conditions for a geodesic to bounce in the region $\frac{1}{t_0} - \varepsilon < t < \frac{1}{t_0}$. Again we know it cannot bounce for $t > \frac{1}{t_0}$ and we want it to bounce before it gets cut off by the next Kasner epoch at $t = \frac{1}{t_0} - \varepsilon$. This is what gives us an upper bound for the geodesic's constant corresponding to the negative value of p_i. Let's suppose that $p_1 < 0$ (the analysis for the other cases would again be similar). Again we want there to be some T in the range $\frac{1}{t_0} - \varepsilon < T < \frac{1}{t_0}$ such that:

$$\frac{M_1^2}{T^{2p_1(u-2)}} + \frac{M_2^2}{T^{2p_2(u-2)}} + \frac{M_3^2}{T^{2p_3(u-2)}} < 1 \tag{5.12}$$

And this again gives us that:

$$\frac{M_1}{T^{2p_1(u-2)}} < 1 \tag{5.13}$$

If we take $S = \frac{1}{T}$ then we have that:

$$M_1 < S^{(-p_1(u-2))} \tag{5.14}$$

and as $T > \frac{1}{t_0} - \varepsilon$, then:

$$S < \frac{t_0}{1 - \varepsilon t_0} \tag{5.15}$$

So combining these inequalities we get that:

$$M_1 < \left(\frac{t_0}{1 - \varepsilon t_0}\right)^{(-p_1(u-2))} \tag{5.16}$$

However, like the previous inequalities, this is required to be satisfied for a geodesic to bounce but satisfying the inequalities doesn't guarantee that the geodesic will bounce.

5.4 Plotting the Bouncing Region

To summarise the previous sections, we have derived four inequalities that are are needed for a geodesic to bounce when a transition occurs ε away from the regular transition time. Namely:

$$M_2 < \left(\frac{1}{t_0}\right)^{p_2(u-2)} \tag{5.17}$$

$$M_3 < \left(\frac{1}{t_0}\right)^{p_3(u-2)} \tag{5.18}$$

$$M_1 < \left(\frac{t_0}{1-\varepsilon t_0}\right)^{(-p_1(u-2))} \tag{5.19}$$

$$1 < M_1^2 + M_2^2 + M_3^2 \tag{5.20}$$

It is possible to have a geodesic which satisfies these inequalities. This region can be plotted but we can see from the equations that it basically gives us a square of M_i-space with the unit sphere cut out producing plots like figure 5.2. This is the region of M_i-space satisfying those inequalities with $u = \sqrt{7}$, $t_0 = 2$ and $\varepsilon = 0.1$. We can see that it is a comparatively very small region of the space (as for simplicity we have not compactified the M_i in the preceding analysis) in which it is possible for such geodesics exist.

However, we must be careful to emphasise that what we have shown, is that if there are any bouncing geodesics, they must lie in this region but the converse is not necessarily true. Not all points in this region are going to give geodesics which exhibit bouncing.

So it appears that if we have three Kasner epochs, all is not totally lost for geodesics to bounce after the first epoch. But if we add more and more epochs, the sheer number of parameters in our model make the analysis (both numerical and analytical) more and more difficult. So we are going to simplify the situation by reducing the number of parameters and considering geodesics which we will call "initially purely K_1". By this, we mean that in the first epoch, these geodesics have only one non-zero constant and that is in the spatial direction which has a negative power.

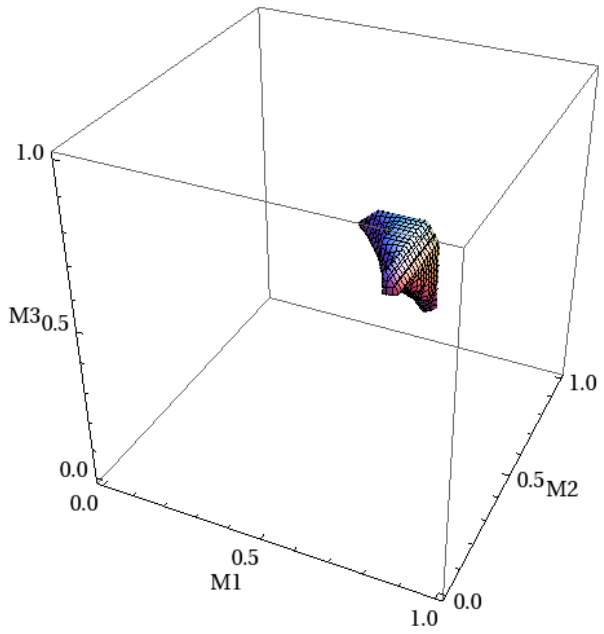

Figure 5.2: An example of the region in M_i-space in which it may be possible to find bouncing geodesics.

5.5 Initially Purely K_1 Geodesics

We are going to study geodesics which are initially purely K_1 in a little more detail now. These geodesics start with a potential of the form

$$V(t) = 1 - K_1^2 t^{(-2p_1)} \tag{5.21}$$

As a pure K_1 geodesic evolves through the Kasner epochs towards $t = 0$, the value and (more importantly) the sign of p_1 changes and so the geodesic changes between being effectively purely K_1, K_2 or K_3 depending on the evolution of p_1. Recall from chapter 3 that geodesics with only one non zero constant correspond to potentials which are either increasing (pure K_1) or decreasing (pure K_2 or K_3), if we are looking backwards in time towards $t = 0$. This means that the potential of this geodesic will be a piecewise construction of these increasing and decreasing potentials. So a geodesic which starts as purely K_1 can only bounce in epochs where the potential is increasing i.e. when its non-zero constant corresponds to the contracting direction and it is effectively what we are calling purely K_1. Looking at purely K_1 geodesics

massively simplifies the conditions for geodesics bouncing because as the potential is always either strictly increasing or strictly decreasing, we only need to evaluate the potential at the transition times t_i. As soon as one of $V(t_i)$ becomes positive we know that the geodesic has bounced in the preceding epoch. So in order to determine whether or not a geodesic bounces we only need to evaluate the sequence $V(t_i)$ and see if it ever becomes positive. We also know from (3.12) that in a Kasner metric with parameter p_1, the pure K_1 geodesic bounces at time $(K_1)^{\frac{1}{p_1}}$

5.5.1 One Situation

Lets look at one example of a situation where we could get geodesic bouncing occurring. Suppose we have the following set-up (illustrated in figure 5.3). We take a set of n Kasner epochs within the Mixmaster Universe and give it a scheme of time transitions where all transitions occur in log regular time except for the last (i.e. the one closest to the singularity). We will call the potential in the last epoch V_1 and the potentials in the preceding epochs will be V_2, V_3 etc. (so the potential of the geodesic is a piecewise combination of these potentials). We will scale the transition time scheme so that if it were regular, this last transition would occur at $t = 1$. So the later transitions will be $\{t_0^i : i = 1, 2, 3 \dots n-1\}$ where t_0 is greater than 1. The epoch where the geodesic potential is V_i will occur between the transition times t_0^{i-1} and t_0^i. However, we are going to make the epoch closest to the singularity a little bit longer than it would be. So the last transition will actually occur at $t = 1 - \varepsilon$. We assume that the geodesic has not bounced previously and so by our theorem, the first interval in which it can bounce is $1 - \varepsilon < t < 1$. As we are still considering geodesics which have only one non-zero constant then any geodesic which bounces in this region must be pure K_1 in this epoch.

The pure K_1 geodesics which bounce in this region are the ones in the range:

$$1 < K_1 < \left(\frac{1}{1-\varepsilon}\right)^{(-p_1)} \tag{5.22}$$

by (3.12). (Here K_1 is the value of the constant in the epoch in which the bouncing occurs.) So for pure K_1 geodesics, a range of times in which it is possible for them to bounce corresponds to an interval on the K_1 axis. Now we also want this geodesic

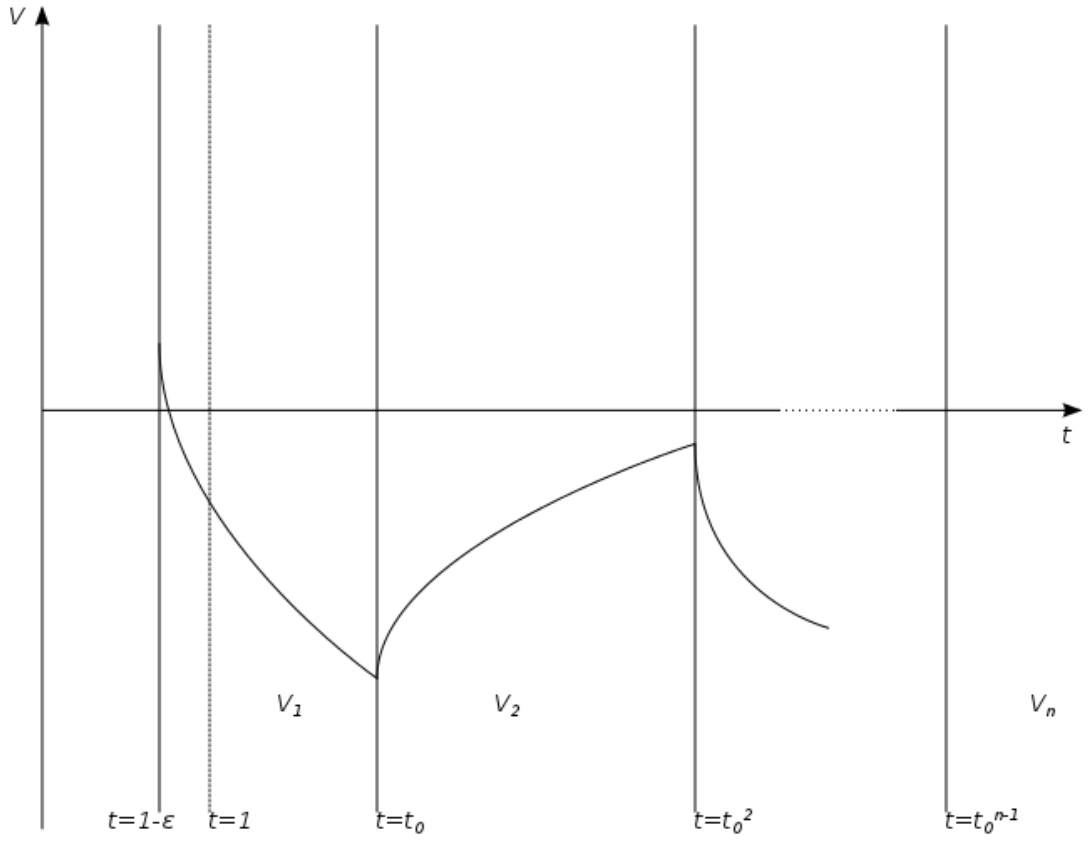

Figure 5.3: A sketch of a potential in a mixmaster universe with nearly regular transition times demonstrating how it may be possible for a geodesic in such a setup to bounce.

not to have bounced in any of the previous epochs. So we are going to have to evolve this constant through the previous epochs. In order to do that we are going to label the constant for this geodesic in the ith epoch to be $K_{1[i]}$ and the parameter in the Kasner metric in the ith epoch to be $p_{1[i]}$ (noting that this may be either positive or negative - here we are using the subscript 1 to show that it is the parameter in the same direction as K_1). So $K_{1[1]} = K_1$ in the range above. Now we know from (4.4), that

$$K_{1[n]} = \left(t_0^{(n-1)}\right)^{(p_{1[n]} - p_{1[n-1]})} K_{1[n-1]} \tag{5.23}$$

Applying this repeatedly gives us that in terms of $K_{1[1]}$, $K_{1[n]}$ is given by:

$$K_{1[n]} = t_0^{(np_{1[n]} - \sum_{i=1}^{n} p_{1[i]})} K_{1[1]} \tag{5.24}$$

Now all that we require for a geodesic not to bounce in any of the previous epochs, is for the potential to be negative at all previous transition times. But this only requires that it be negative for the first transition as then by our theorem it remains negative for all others. So we need:

$$\begin{aligned} V_n(K_{1[n]}, t_0^{n-1}) &< 0 && (5.25)\\ 1 - \frac{K_{n[1]}^2}{(t_0^{n-1})^{(2p_{1[n]})}} &< 0 && (5.26)\\ K_{1[n]} &> t_0^{(n-1)p_{1[n]}} && (5.27) \end{aligned}$$

So these are the geodesics which don't bounce in the first epoch. So we have a set of geodesics which don't bounce in the first epoch and an interval of geodesics which DO bounce in the last epoch (which is ε longer than expected). So in terms of $K_{1[1]}$, the above inequality is:

$$t_0^{(np_{1[n]} - \sum_{i=1}^{n} p_{1[i]})} K_{1[1]} > t_0^{(n-1)p_{1[n]}} \tag{5.28}$$

which simplifies to

$$K_{1[1]} > t_0^{\sum_{i=1}^{n-1} p_{1[i]}} \tag{5.29}$$

So this is the condition on $K_{1[1]}$ for the geodesics not to have bounced before the last epoch. So to have some geodesics bouncing in this last epoch which have not bounced previously, then we require that there be some $K_{1[1]}$ in the region:

$$t_0^{\left(\sum_{i=1}^{n-1} p_{1[i]}\right)} < K_{1[1]} < \left(\frac{1}{1-\varepsilon}\right)^{(-p_1)} \tag{5.30}$$

i.e. we certainly need that all the relevant parameters satisfy:

$$t_0^{\left(\sum_{i=1}^{n-1} p_{1[i]}\right)} < \left(\frac{1}{1-\varepsilon}\right)^{(-p_1)} \tag{5.31}$$

Let's look at this inequality in a little more detail as it is only based on the parameters of the model. Firstly we have chosen $p_{1[1]}$ to be negative and we must have $\varepsilon < 1$ (as otherwise the last transition would occur at $t < 0$ which we can't have). So the right hand side of the inequality must be greater than 1. We also have that $t_0 > 1$, so whether or not this inequality is satisfied depends entirely on the set of parameters $p_{1[i]}$. In order to make this region is large as possible, it means that

we want the sum of the $p_{1[i]}$ to be as small as possible. This implies that we would like as many of the $p_{1[i]}$ to be negative as possible to maximise the length of the region of bouncing geodesics. This intuitively makes sense as in these regions, the potential is increasing (towards the singularity) so the more time it is increasing, the more likely it is to hit zero and thus the geodesic bounces.

So in this (somewhat contrived) situation, it is certainly possible to have some bouncing geodesics and it seems to lead us to conjecture that whether or not we can have initially purely K_1 geodesics bouncing very much depends on how often the geodesic's constant is in the same direction as the negative power in the metric.

As it seems that it is possible for geodesics to bounce in a model with more irregular time transitions, it means we want to do some kind of probabilistic analysis for on average how much bouncing occurs in a mixmaster universe with a set of irregular time transitions. In the next section we will look at what happens when all our transitions are shifted outside the regular time scheme and we try to determine the average amount of bouncing which occurs in this scenario.

5.6 Average Length of Bouncing Region in Pure K_1 Geodesics

We have shown that it is possible for geodesics which are pure K_1 to bounce in some scenarios where we have irregular time transitions but not necessarily in all of them. So we would like to measure how the bouncing region depends on the set of ε's away from the regular transitions. To do that we are going to recast the transitions as:

$$s_i = i \log \frac{1}{m} + \varepsilon r_i \tag{5.32}$$

where $t = e^s$ so we are working in logarithmic time. The set $\{r_i\}$ will be a set of random numbers between -1 and 1 with a uniform distribution. The reason we are doing these calculations in logarithmic time is because we are randomly generating values of $\{r_i\}$. If we kept the transition times in terms of a geometric series, then

the randomly produced perturbations are likely to cause the transition times close to the singularity to overlap, which will cause difficulties in generating the piecewise potential for the computer. Starting out with regularly spaced transitions makes this much less likely to happen. So with this set of transitions, we then can vary ε and by finding the bouncing region for many sets $\{r_i\}$, we can get an average bouncing length depending on ε. As we are again looking at pure K_1 geodesics, all that we need to do to find the value of the potential at each of the transition times (recall that for these geodesics the potential is either monotonically increasing or decreasing in each epoch). Then we know that the first time the potential is positive at a transition, the geodesic has bounced in the preceding epoch.

We are again going to have to pick a particular initial u for the mixmaster universe and for this we have chosen u to be $\sqrt{101}$ initially and we are using 10 epochs in this particular example. This means that the value of u remains above 1 throughout the evolution which in turn means that the potential is increasing in half of the epochs and decreasing in the other half.

If there are any geodesics bouncing after the first epoch, we know that for each epoch, there will be an interval in k_1-space (we are compactifying the K_i using the same compactification as before 3.18) corresponding to these geodesics. Again this will be done using a Mathematica although we are not actually solving anything numerically. Mathematica is needed to generate the sets $\{r_i\}$ and do a large number of tests. We use a series of test points from $k_1 = 0.01$ to $k_1 = 0.99$ at intervals of 0.0001 and use these to measure the length of each interval in each epoch by finding at which of the transition times the potential first becomes positive (as then we know that the geodesic has bounced in the preceding epoch). We can then add up these intervals to get a length for the region where geodesics bounce after the first epoch. This takes a reasonable amount of time for each run as we are sampling quite a lot of points but this is necessary as some of the intervals of bouncing are very small and this separation of test points was found to be the best compromise between running time and finding very small regions of bouncing.

ε	Mean	Standard Deviation
0.01	0.00023	0.00037
0.02	0.00068	0.00097
0.03	0.0013	0.0017
0.05	0.0030	0.0035
0.07	0.0042	0.0051
0.1	0.007	0.0085
0.15	0.011	0.013
0.2	0.015	0.017
0.3	0.022	0.023
0.4	0.031	0.030
0.5	0.039	0.041
0.6	0.048	0.047

Table 5.1: The mean length of the region of the k_1-axis corresponding to geodesics which bounce after the first epoch for varying parameter ε.

This was done for a range of ε from 0.01 to 0.6, and the mean bounce length and standard deviation for each ε was calculated. The results are shown in the table 5.1 below and these were then plotted figure 5.4. They appear to show a clear linear dependence between ε and the length of the bouncing region. The line has been fit to the results, it has equation:

$$y = -0.000848008 + 0.0799846x \tag{5.33}$$

We can also ask for each ε, what proportion of sets of $\{r_i\}$ give a region of bouncing after the first epoch? For each ε we look at the proportion of sets $\{r_i\}$ which have a region of bouncing beyond the first epoch in k_1 space. This is shown in the second table 5.2.

From this table it seems that as we increase ε, the proportion of sets of perturbations which show bouncing after the first epoch increases. It also seems that the proportion of random sets showing later bouncing is quite high so it appears that

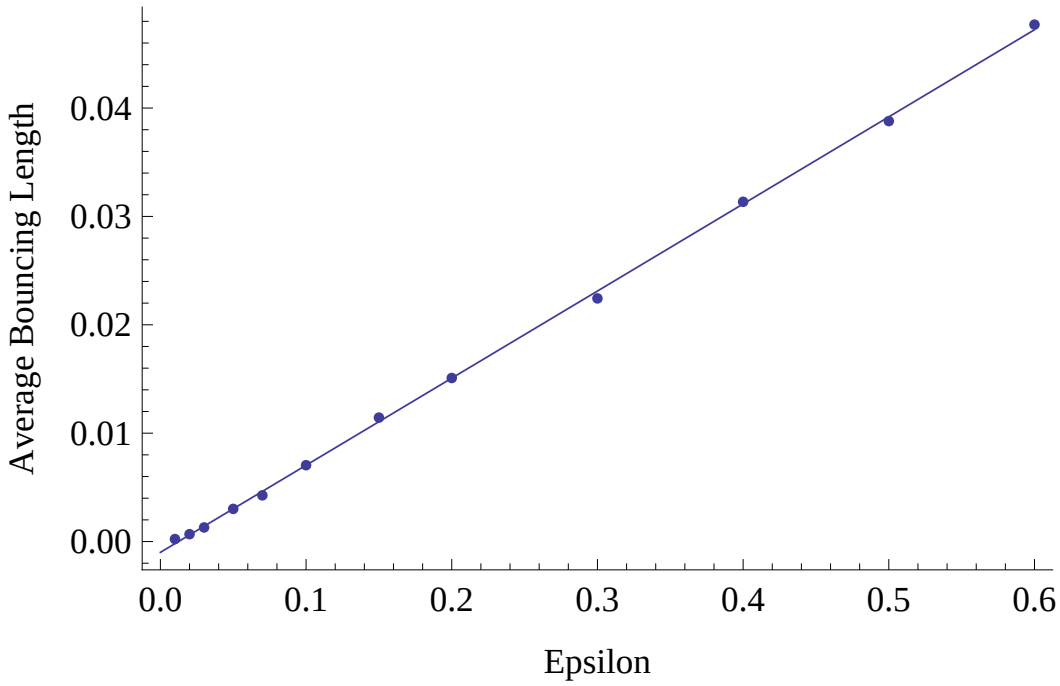

Figure 5.4: A plot of the average length of the region of bouncing geodesics versus ε with $u = \sqrt{101}$.

with random perturbations away from a regular transition scheme (regulated by ε), the chances of seeing bouncing geodesics in later epochs is quite likely but the set of such geodesics will be relatively small.

5.6.1 Different Initial Values of u

In the previous section we saw that it was possible to have geodesics bouncing after the first transition in the first ten epochs where the value of u never drops below 1 (so we were only looking at one era in the mixmaster universe). But what happens if we change the initial value of u such that it does drop below 1? This means that the potential is decreasing in more than half the epochs and increasing in less than half so intuitively we might expect there to be less bouncing in this situation.

Indeed this turns out to be the case. We are going to investigate a few different situations. First we are going to set $u = \sqrt{101} - 3$ initially. This means that going from the seventh to the eighth epoch, the value of u drops below 1 and we enter a different era. The p_i evolve such that for the last three epochs, p_1 is positive and

ε	Proportion of r_i sets with late bouncing
0.01	0.54
0.02	0.65
0.03	0.63
0.05	0.79
0.07	0.72
0.1	0.70
0.15	0.75
0.2	0.72
0.3	0.81
0.4	0.78
0.5	0.78
0.6	0.80

Table 5.2: This table shows the proportion of sets of random perturbations in the transition times which show bouncing after the first epoch

hence it is impossible for pure K_1 geodesics to bounce in any of these epochs. As expected then, when we work out the average bouncing length for different ε, we find that it is smaller. The results for the mean bouncing length with varying ε are plotted in figure 5.5. The line of best for this value of u was given by:

$$y = -0.00097819 + 0.0731634x \tag{5.34}$$

So the gradient is lower but not by much. This is what we would expect at some level because we are cutting off any opportunity for the geodesics to bounce in the last three epochs as here an initially pure K_1 geodesic is effectively pure K_3 so cannot bounce in any of these epochs. Also the fact that the difference between this example and that when $u = \sqrt{101}$ is quite small is also not surprising as the length of the bouncing region contributed by these later epochs in the $u = \sqrt{101}$ is comparatively small.

But what happens if we have an initial value of u which goes through three

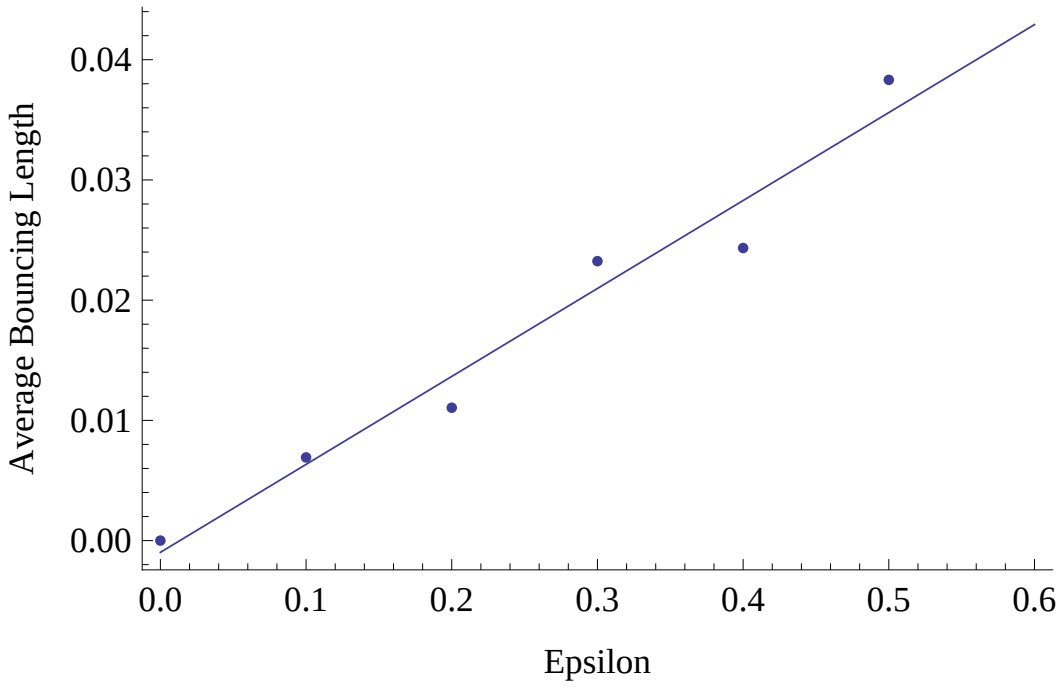

Figure 5.5: A plot of the average length of the regions of bouncing geodesics versus ε with $u = \sqrt{101} - 3$.

eras so that the contracting direction comes back to coinciding with the direction of K_1. This would mean that it would be theoretically possible for an initially pure K_1 geodesic to bounce in this third era. A contrived example was found that by setting $u = \sqrt{10} + 0.16$, then the sign of p_1 goes through the following evolution $-, +, -, +, +, +, +, -, +, -$. In this scenario, it would be theoretically possible for pure K_1 geodesics to bounce in epochs 1, 3, 8 and 10. So the average length of bouncing after the first epoch for varying ε was found with this value of u and the results plotted in figure (5.6). This showed an even lower average bouncing length. The line of best fit for this graph is $y = -0.00113759 + 0.0376241x$ so this has a much shallower gradient. In fact, it was noticed in these results, that the only epochs in which bouncing occurs are the first and the third. Once the relevant p_1 has been positive for the next four epochs, it seems that it is impossible for any of the geodesics to bounce in the epochs after this. This is again consistent with our conjecture that whether geodesics bounce depends strongly on how often their constant is in the same direction as the negative power in the metric. If there are a sequence of epochs where the corresponding power in the metric is always positive, the poten-

tial gets "knocked down" too low for the subsequent period of increasing to rescue it.

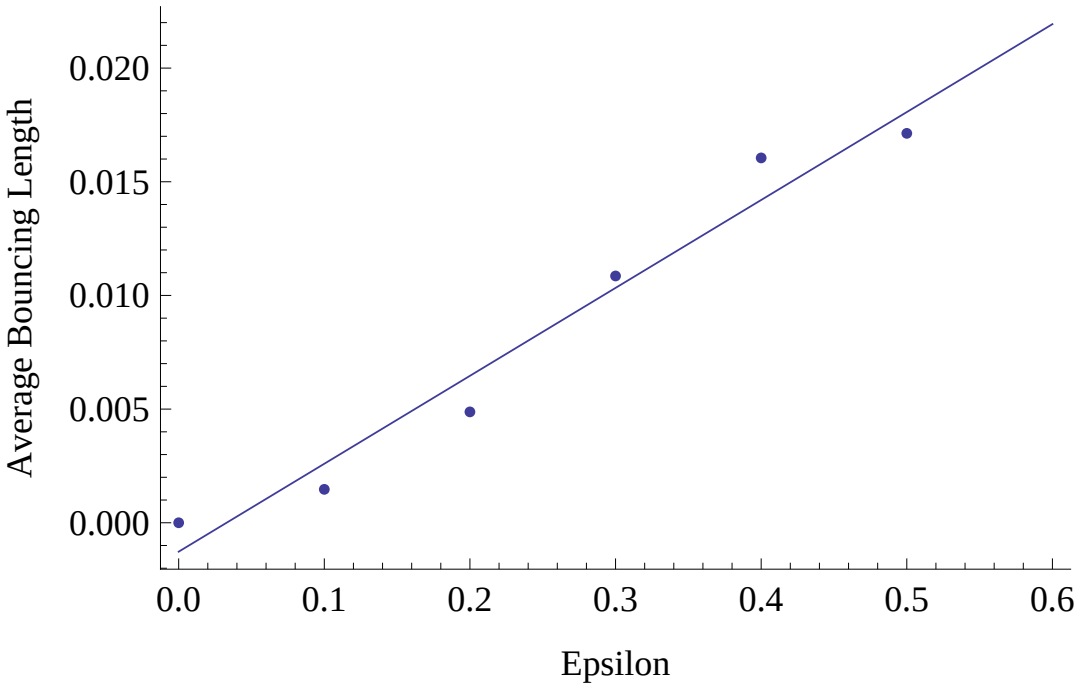

Figure 5.6: A plot of the average length of the region of bouncing geodesics versus ε, $u = \sqrt{10} + 0.16$.

The other value of u tried was to set $u = \varphi = \frac{1+\sqrt{5}}{2}$. Noting that this value of u remains constant throughout the evolution and is such that the contracting direction permutes between all three axes (a point which will be mentioned again in chapter 6), it essentially corresponds to each era being of length 1. It means that K_1 is in the contracting direction for $\frac{1}{3}$ of the epochs. It was found that when this was taken as the initial u, it seems that no bouncing occurred for any value of $\varepsilon \lesssim 0.5$.

The results seem to suggest that introducing random perturbations in the time transitions give some purely K_1 geodesics the opportunity to bounce in the first era but that when the next era is entered so that the direction corresponding to K_1 is always expanding for some set of epochs, this knocks the potential too far down for the later perturbations to compensate enough to bring the potential back to zero when it is increasing again and so the geodesics can no longer bounce after this point.

This means that in some sense, the integer part of the initial value of u gives us a measure of how close to the singularity we can get bouncing geodesics.

5.7 Summary

We have shown in this chapter that if the set of transition times in our model of the mixmaster universe is perturbed around the regular transition times, then this can allow spacelike geodesics to bounce after the first epoch in certain situations. But even in these contrived scenarios, the proportion of bouncing geodesics is fairly small. It also seems possible to have initially purely K_1 geodesics bouncing after the first epoch but that these appear to be prohibited from bouncing after the end of an "era". This seems to imply that it is extremely difficult if not impossible to get geodesics bouncing in the full mixmaster universe where we have an infinite number of epochs and eras. Indeed, according to [20], stochastic analysis of the long-term replacements of the epochs and eras implies that the majority of the u values are very large. This suggests that the eras will correspondingly be very long. This is calamitous for our pure K_1 bouncing geodesics as it means there will be long eras where the potential will be decreasing thus making it near impossible for the potential to increase to zero even when the potential is increasing. Any given geodesic would have to be extraordinary lucky for the time transitions and parameter evolution to work out in such a way that it bounces back close to the singularity.

Chapter 6

The Puzzle of a Periodic Parameter

There now follows a digression away from the discussion of geodesics to investigate a curious aspect of the evolution of the Mixmaster Universe. This was noticed through looking at many initial values of the parameter u by which to run the numerical calculations for the geodesics. In fact, the requirement that the initial u be irrational for the mixmaster evolution to continue infinitely meant that it seemed sensible to take square roots of integers as initial values of u. Observing the evolution of these through the Kasner epochs showed that taking this parameter to initially be a square root led to it becoming periodic through the evolution of the metric. The potential for such periodic values to exist is mentioned in [23] and it was discovered while writing this thesis that some extensive work on this subject had also been done by Cornish and Levin in [26] but was done differently to how we will discuss it here. We are going to use some comparatively simple mathematics to demonstrate that the mixmaster universe exhibits some very complicated behaviour.

Recall from chapter 2 that the parameters $\{p_i\}$ in the metric of the mixmaster universe could be written in terms of a parameter u (2.6). The evolution through the various Kasner epochs of the mixmaster universe was given by the evolution of

n	2	3	5	6	7	8	10	11	12	13
Period	2	3	4	6	7	5	6	9	8	10

Table 6.1: A table of length of the periods of u with initial $u = \sqrt{n}$

this parameter as follows: if we start with an initial value u_0, then:

$$u_{i+1} = \begin{cases} u_i - 1 & u_i - 1 > 1 \\ \frac{1}{u_i - 1} & u_i - 1 < 1 \end{cases} \tag{6.1}$$

6.1 Square Roots

It was noticed that if one takes the initial value of the parameter u to be the square root of a natural number (while keeping the constraint that this be irrational) and observe the evolution of u through the rule prescribed above then eventually it seems that u will return to this initial value. For example, if we take $u_0 = \sqrt{6}$ then the u evolves through the following values:

$$u_0 = 2.44949 \to 1.44949 \to 2.22474 \to 1.22474 \to 4.44949 \to 3.44949 \to 2.44949$$

So if u is initially $\sqrt{6}$ then u is periodic with period 6. The natural question to arise from this is: can we prove that all (irrational) square roots lead to periodic values of u?

It might be illuminating to see if there is any obvious relation between the value of u_0 and the period of u given that initial value. Let $u_0 = \sqrt{n}$ and let's look at the value n against the period of u (table 6.1).

Unfortunately, this does not seem to yield any obvious relation so some more investigation is required. So we look at how the parameter u evolves in a little more detail.

6.1.1 The Simplest Scenario

Suppose we start with $u_0 = \sqrt{n}$ where $n \in \mathbf{N}$ and we follow the evolution scheme (6.1), then u drops below 1 after $\lfloor\sqrt{n}\rfloor$ steps in the evolution. So

$$\begin{aligned} u_{\lfloor\sqrt{n}\rfloor} &= \frac{1}{\sqrt{n} - \lfloor\sqrt{n}\rfloor} \\ &= \frac{\sqrt{n} + \lfloor\sqrt{n}\rfloor}{n - \lfloor\sqrt{n}\rfloor^2} \end{aligned} \tag{6.2}$$

where $n - \lfloor\sqrt{n}\rfloor^2 \in \mathbf{N}$. Now the simplest case to consider is if $n - \lfloor\sqrt{n}\rfloor^2 = 1$ for then

$$u_{\lfloor\sqrt{n}\rfloor} = \sqrt{n} + \lfloor\sqrt{n}\rfloor \tag{6.3}$$

and so $u_{2\lfloor\sqrt{n}\rfloor} = \sqrt{n}$. So this value of u would be periodic with period $2\lfloor\sqrt{n}\rfloor$. The condition is satisfied when $n = k^2 + 1$ for some $k \in \mathbf{Z}$. So we have found one class of periodic values of u, those of the form $\sqrt{k^2+1}$.

However, if $n - \lfloor\sqrt{n}\rfloor^2 \neq 1$, further analysis this way becomes leads to very complicated equations very quickly. So a different method is needed to investigate the periodic values.

6.2 The Golden Ratio

At this stage another point of interest, and slight further complication, is introduced. If u is either initially, or at some stage evolves to, the value of the "golden ratio" ($\varphi = \frac{1+\sqrt{5}}{2} = 1.618\ldots$) then it remains constant at this value for all subsequent Kasner epochs. This is because u satisfies the equation:

$$u = \frac{1}{u - 1} \tag{6.4}$$

which is the identity by which the golden ratio φ is defined. This is another periodic value of u (which has period 1) which is not just a square root of an integer. This raises another question. Are there more periodic values of u which are not just simple square roots?

6.3 How to Generate Some Periodic Values

We are going to attempt to generate some periodic values of u by using the equations for its evolution, to find the equation that such a value would satisfy. So we define two functions

$$f_1(u) = u - 1 \tag{6.5}$$

$$f_2(u) = \frac{1}{u-1} \tag{6.6}$$

As u evolves from one Kasner epoch to the next, we have either $u \to f_1(u)$ or $u \to f_2(u)$ depending on whether u is larger than 2 or not. So if we begin with some general value of u we can generate all the possible evolutions of u by composing these functions in all possible combinations. A periodic value of u is obtained when the composition of these functions returns the initial value of u. This way we can classify the periodic values by their periods. So the u with period 1 solves the equation $f_2(u) = u$, those with period 2 satisfy the equations $f_2 \circ f_1(u) = u$, $f_2 \circ f_2(u) = u$, $f_1 \circ f_2(u) = u$ and so on. This means for period n, we get $2^n - 1$ equations (as clearly the equation $f_1 \circ f_1 \circ \ldots \circ f_1(u) = u - n = u$ has no solution). These were generated on a computer up to $n = 20$ and are shown that when simplified they become quadratic equations with integer coefficients. We can plot the periodic values of u such quadratics generate by their period (figure 6.1).

6.3.1 Largest and Smallest Periodic Values

Generating the periodic values (again up to period 20) by computer, and the quadratic equations which seem to generate them shows that the largest periodic value of period n is given by the positive solution to the equation:

$$1 + nu - u^2 = 0 \tag{6.7}$$

This gives the largest periodic value with period n as:

$$u = \frac{n + \sqrt{n^2 + 4}}{2} \tag{6.8}$$

The smallest periodic value is the positive solution to the equation:

$$n - (n-2)u - u^2 = 0 \tag{6.9}$$

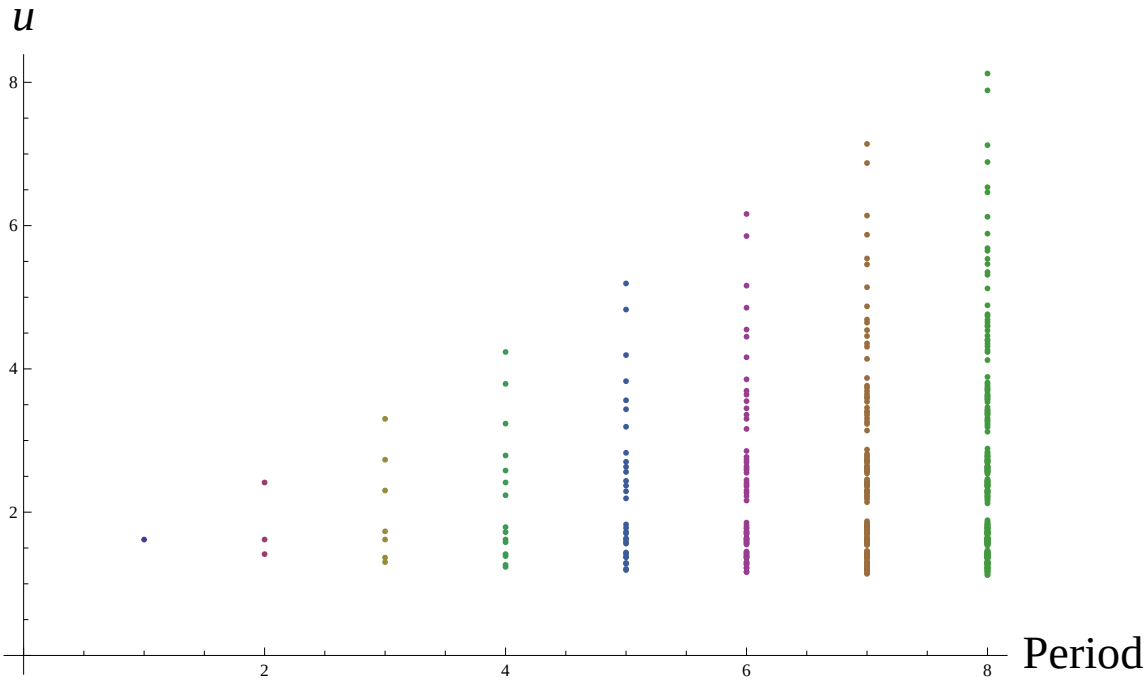

Figure 6.1: A plot of the periodic values of u plotted by period

which gives the smallest value of u with period n as:

$$u = \frac{(2-n) + \sqrt{n^2+4}}{2} \tag{6.10}$$

From these we can see that the largest periodic value goes like n as n gets large and the smallest value goes to 1 as n gets large. This confirms what is seen in the graph (figure 6.1) and shows that we can have periodic values as large as we like.

6.3.2 Generating Quadratics

Indeed it can further be shown that all possible u's which are periodic solve a quadratic equation. First we prove the following result:

Proposition 2 *Any length composition of f_1 and f_2 gives a function of the form:*

$$f_{i_1} \circ f_{i_2} \ldots f_{i_n}(u) = \frac{au+b}{cu+d} \tag{6.11}$$

with $ad - bc = \pm 1$ where $i_1, \ldots i_n \in \{1, 2\}$ and $a, b, c, d \in \mathbf{Z}$.

Proof 2 *The argument is by induction. Suppose $H(u) = f_{i_1} \circ f_{i_2} \ldots f_{i_n}(u) = \frac{au+b}{cu+d}$, then the two functions formed from this are $f_1 \circ H(u)$ and $f_2 \circ H(u)$.*

First consider $f_1 \circ H(u)$*:*

$$\begin{aligned} f_1 \circ H(u) &= \frac{au+b}{cu+d} - 1 \\ &= \frac{a+bu-(c+du)}{c+du} \\ &= \frac{(a-c)+(b-d)u}{c+du} \end{aligned} \tag{6.12}$$

which is of the required form and $(a-c)d-(b-d)c = ad-bc = \pm 1$*.*
Similarly:

$$\begin{aligned} f_2 \circ H(u) &= \frac{1}{\frac{au+b}{cu+d} - 1} \\ &= \frac{c+du}{(a-c)+(b-d)u} \end{aligned} \tag{6.13}$$

which is again the correct form and $c(b-d)-d(a-c) = bc-ad = \mp 1$*.*
As we have:

$$u = \frac{1.u+0}{0.u+1} \tag{6.14}$$

This is of the correct form so by induction, all subsequent functions of u *formed from* f_1 *and* f_2 *have this form.*

This then leads to the following result.

Proposition 3 *If* u *is periodic then* u *satisfies a quadratic equation with integer coefficients.*

Proof 3 *If* u *is periodic then we must have that* $H(u) = u$ *(where* H *is composed of the functions* f_1 *and* f_2 *as in the previous proposition). As this means*

$$H(u) = \frac{au+b}{cu+d} = u \tag{6.15}$$

with $a, b, c, d \in \mathbf{Z}$*. Simplifying this gives* $cu^2 + (d-a)u - b = 0$ *as required.*

It has been shown that periodic values of u are given by solutions to the equation $cu^2 + (d-a)u - b = 0$ with the condition that $ad - bc = \pm 1$. The questions this naturally raises are:

- Do all such quadratics lead to a periodic value of u?
- If not, what subset of these quadratics are being generated by f_1 and f_2?

6.3.3 Some Observations

It is important to note that the values of u generated do evolve the same way as their generation scheme. So the periodic value generated by the equation $f_1 \circ f_1 \circ f_2(u) = u$ say, does indeed follow the evolution $u \to f_2(u) \to f_1(f_2(u)) \to f_1(f_1(f_2(u))) = u$. Also note that each of the values u evolves through are themselves other periodic values of u. Indeed they correspond to the equations that are cyclic permutations of the one for the original u. So in the example, they would be the solutions to equations $f_2 \circ f_1 \circ f_1(u) = u$ and $f_1 \circ f_2 \circ f_1(u) = u$. Also note that the equations formed from n applications of f_1 and f_2 do not necessarily all give values of u with period n but are only required to have a period m which divides n.

6.4 Further Investigation of the Quadratics

We have shown that the periodic values of u are found through solutions of quadratic equations and we would like to investigate these equations in a little more detail. As mentioned before, we can use Mathematica to generate these quadratics in the form $c + bu + au^2 = 0$. (Note that the coefficients a, b, c are different from previous sections). We can then plot these in $\{a, b, c\}$-space. This is shown in figure 6.2 where the different coloured points correspond to the size of the period of that equation's solution.

But this picture doesn't give much insight. It is much more interesting to divide the quadratics by the coefficient of u^2 so they have the form $u^2 + bu + c = 0$ and plot them in 2 dimensional $\{b, c\}$-space (figure 6.3). This plots the coefficients of the quadratics corresponding to values of u with period up to 13.

Here we can see a much more interesting structure emerging. By zooming in on a region, we can see that the plot appears to have a fractal nature (figure 6.4) in the sense that the plot appears to exhibit a self similar structure.

We can look at how the fractal evolves by plotting the coefficients for different maximum periods. In figure 6.5, we plot the evolving fractal for period 5 (i), 7 (ii), 9 (iii) and 11 (iv).

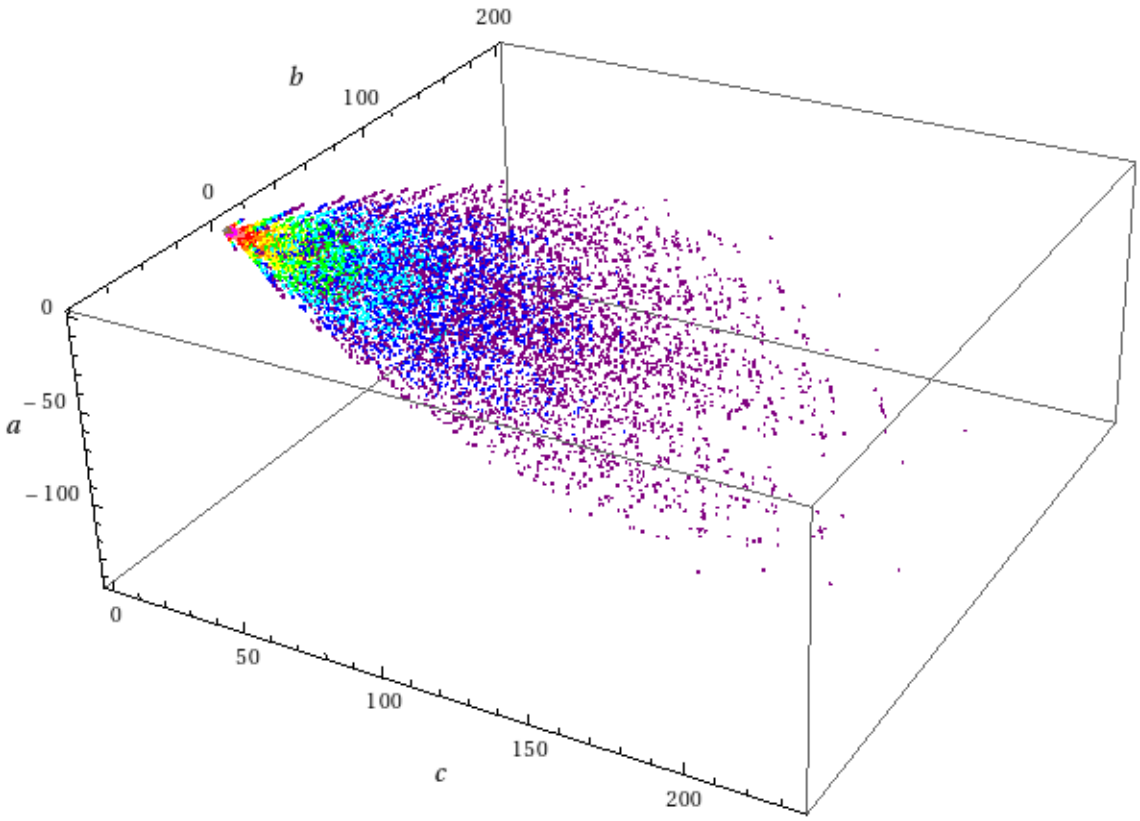

Figure 6.2: A three dimensional plot of coefficients of quadratics whose solutions give periodic values of u.

6.5 Generation Via Matrices

Another way to look at the quadratics generated by the functions f_1 and f_2 is to translate them into matrices. It was hoped that doing this might give insight as to what set of quadratics we are producing in the fractal pictures. We have shown that any composition of these functions can be written $\frac{au+b}{cu+d}$ where a,b,c,d are integers satisfying the relation $ad - bc = \pm 1$. We can write this as the matrix

$$\begin{pmatrix} a & b \\ c & d \end{pmatrix} \tag{6.16}$$

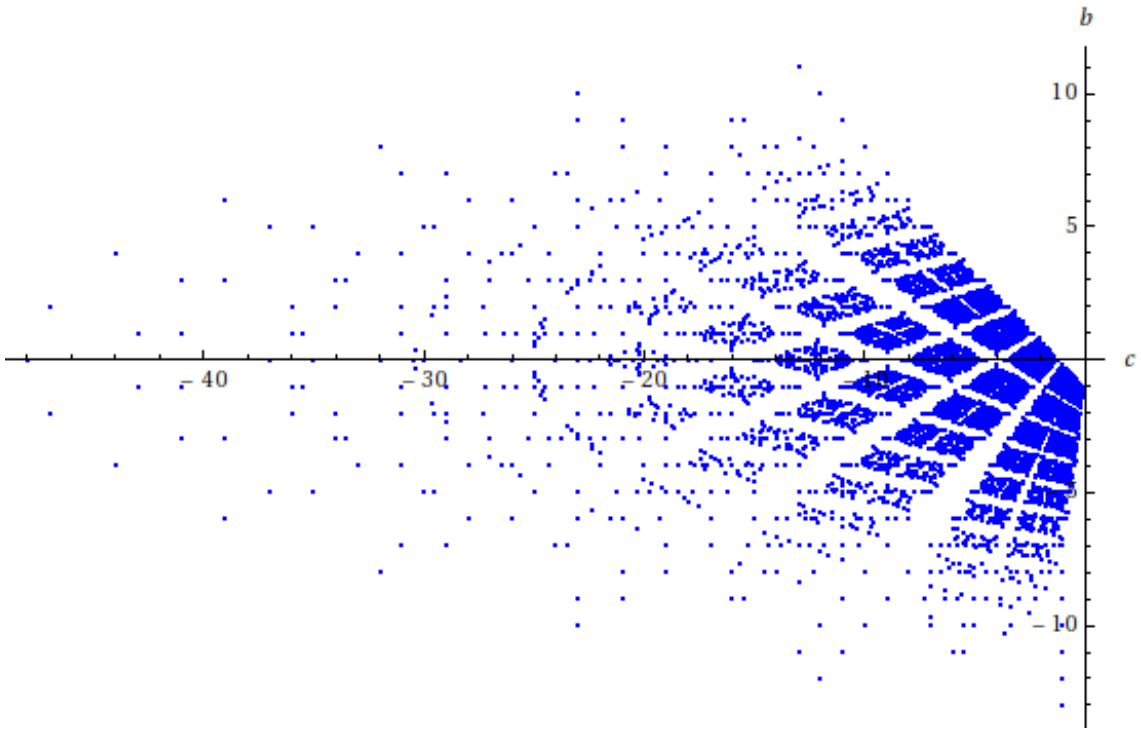

Figure 6.3: A two dimensional plot of coefficients of quadratics whose solutions give periodic values of u.

which has determinant ± 1. We can then translate the functions f_1 and f_2 into matrices. They become:

$$f_1 = \begin{pmatrix} 1 & -1 \\ 0 & 1 \end{pmatrix} \tag{6.17}$$

$$f_2 = \begin{pmatrix} 0 & 1 \\ 1 & -1 \end{pmatrix} \tag{6.18}$$

and composing the functions is equivalent to matrix multiplication (on the left). In this set-up the initial u is just the identity matrix. Now, in order to find out which quadratics we are generating, we want to find which matrices are generated by f_1 and f_2. In particular, is it possible to generate any matrix with determinant ± 1 with these two matrices?

A general matrix M generated by f_1 and f_2 has the form

$$M = f_1^{i_1} f_2^{i_2} f_1^{i_3} \dots f_2^{i_k} \tag{6.19}$$

where $i_1, i_2 \dots i_k \in \mathbf{N} \cup \{0\}$.

First we are going to look at the powers of f_1.

Proposition 4

$$f_1^n = \begin{pmatrix} 1 & -n \\ 0 & 1 \end{pmatrix} \tag{6.20}$$

Proof 4 *By induction. Clearly the proposition is true for $n = 1$. Assume it is true for n. Then:*

$$\begin{aligned} f_1^{n+1} &= f_1.f_1^n \\ &= \begin{pmatrix} 1 & -1 \\ 0 & 1 \end{pmatrix} \begin{pmatrix} 1 & -n \\ 0 & 1 \end{pmatrix} \\ &= \begin{pmatrix} 1 & -(n+1) \\ 0 & 1 \end{pmatrix} \end{aligned}$$

So the proposition is true.

Similarly for powers of f_2.

Proposition 5

$$f_2^n = \begin{pmatrix} (-1)^n F_{n-1} & (-1)^{n+1} F_n \\ (-1)^{n+1} F_n & (-1)^n F_{n+1} \end{pmatrix} \tag{6.21}$$

where F_n is the nth Fibonacci number.

Proof 5 *Again by induction. It is clearly true for $n = 1$. Now*

$$\begin{aligned} f_2^{n+1} &= f_2.f_2^n \\ &= \begin{pmatrix} 0 & 1 \\ 1 & -1 \end{pmatrix} \begin{pmatrix} (-1)^n F_{n-1} & (-1)^{n+1} F_n \\ (-1)^{n+1} F_n & (-1)^n F_{n+1} \end{pmatrix} \\ &= \begin{pmatrix} (-1)^{n+1} F_n & (-1)^n F_{n+1} \\ (-1)^n F_{n-1} + (-1)^{n+2} F_n & (-1)^{n+1} + (-1)^{n+1} F_{n+1} \end{pmatrix} \\ &= \begin{pmatrix} (-1)^{n+1} F_n & (-1)^n F_{n+1} \\ (-1)^{n+2} F_{n+1} & (-1)^{n+1} F_{n+2} \end{pmatrix} \end{aligned}$$

as $F_{n-1} + F_n = F_{n+1}$. And so the proposition is proven.

Note that both these propositions hold for $n = 0$ if we take $F_{-1} = 1$.

Now we want to start looking at what happens when we multiply powers of f_1 and f_2 together.

Proposition 6

$$f_1^n f_2^m = \begin{pmatrix} (-1)^m(F_{m-1} + nF_m) & (-1)^{m+1}(F_m + nF_{m+1}) \\ (-1)^{m+1}F_m & (-1)^m F_{m+1} \end{pmatrix} \tag{6.22}$$

Proof 6 *Trivial matrix multiplication.*

The first thing we can show with this result is that it is definitely not possible to generate *any* matrix using these two generators. From Proposition 5 we can see that

$$f_1^n f_2^m = \begin{pmatrix} (-1)^m A & (-1)^{m+1}B \\ (-1)^{m+1}C & (-1)^m D \end{pmatrix} \tag{6.23}$$

where A, B, C, D are positive integers. Or equivalently:

$$f_1^n f_2^m = (-1)^m \begin{pmatrix} A & -B \\ -C & D \end{pmatrix} \tag{6.24}$$

So the entries on one diagonal have the same sign which is opposite to the sign of the entries on the other. Now, one can show that multiplying two matrices of this type together, one gets:

$$f_1^{n_1} f_2^{m_1} f_1^{n_2} f_2^{m_2} = (-1)^{m_1+m_2} \begin{pmatrix} A_1A_2 + B_1C_2 & -(A_1B_2 + B_1D_2) \\ -(C_1A_2 + D_1C_2) & C_1B_2 + D_1D_2 \end{pmatrix} \tag{6.25}$$

which is of the same form. Therefore any matrix generated by f_1 and f_2 must have the property that entries on the two opposite diagonals have opposite signs. More specifically this prevents us from generating inverses. For a concrete example one can see that:

$$f_1^{-1} = \begin{pmatrix} 1 & 1 \\ 0 & 1 \end{pmatrix} \tag{6.26}$$

As all the entries have positive sign, then it will be impossible to generate this matrix using f_1 and f_2. This makes sense as if one did have:

$$f_1^{-1} = f_1^{i_1} f_2^{i_2} f_1^{i_3} \dots f_2^{i_k} \tag{6.27}$$

then relating it back to finding the periodic values of u, it would mean that the equation

$$f_1(f_1^{i_1} f_2^{i_2} f_1^{i_3} \dots f_2^{i_k})(u) = u \tag{6.28}$$

would be satisfied for any value of u which doesn't really make sense as this is how we are finding periodic values. So these two matrices don't generate a group and the set of quadratics we are generating remain unclear.

6.6 Back to the Square Roots

It would be nice to be able to use these matrices to at least prove the initial observation that taking a square root as the initial value of u gives a periodic evolution. It would seem reasonable that the quadratics whose solutions are exact square roots might be generated in some particular way and hence we could prove that this particular set of quadratics is generated by our matrices and always give periodic solutions. However, this is not quite as straightforward as was hoped. Naïvely one might hope that the periodic value $u = \sqrt{n}$ comes from the quadratic

$$u^2 - n = 0 \tag{6.29}$$

Comparing this with

$$cu^2 + (d-a)u - b = 0 \tag{6.30}$$

would give $c = 1$,$b = n$ and $d - a = 0$. which would seem not to necessarily satisfy the requirement that $ad - bc = \pm 1$ as this implies $a = \sqrt{n \pm 1}$ which may not be an integer. However this is not quite correct. Really, we have that u satisfies the more general equation:

$$k(u^2 - n) = 0 \tag{6.31}$$

so that $c = k$ and $b = nk$ (and $a = d$ as before) requiring us to find an a and k such that

$$a^2 - nk^2 = \pm 1 \tag{6.32}$$

n	Generating formula
2	$f_1 f_2$
3	$f_1 f_2 f_2$
5	$f_1 f_1 f_2 f_1$
6	$f_1 f_1 f_2 f_1 f_2 f_1$
7	$f_1 f_1 f_2 f_2 f_2 f_2 f_1$
8	$f_1 f_1 f_2 f_2 f_1$
10	$f_1 f_1 f_1 f_2 f_1 f_1$
11	$f_1 f_1 f_1 f_2 f_1 f_1 f_2 f_1 f_1$
12	$f_1 f_1 f_1 f_2 f_1 f_2 f_1 f_1$

Table 6.2: A table showing the generating matrices for square root periodic values of u

It seems perfectly reasonable that we should be able to find such integers but even if this is possible, we still haven't shown that our functions f_1 and f_2 will generate these polynomials even if they fit all the constraints (as we have only shown that quadratics that generate the square roots satisfy this constraint, the converse is not necessarily true). So instead, let's see if we can find any patterns in the way the quadratics for square roots are generated from f_1 and f_2 as then it may be possible to work out a general pattern for generating these quadratics from f_1 and f_2. We have shown these in table 6.2.

Unfortunately from this table it does not look like there is any particular way in which these quadratics are generated by f_1 and f_2. So although we can find lots of quadratic equations which we can solve to give periodic values of u, we have yet to determine exactly what subset of the quadratics give us these values.

6.7 Near Periodic Values

It is also interesting to note that each periodic value we can find, comes with an associate infinite class of "nearly periodic" values by which we mean an initial value of u which later evolves into one of the periodic values. So the obvious example

would be a periodic value plus any integer (where the integer is larger than any of the values through which the periodic value evolves in its normal evolution). But there are many more ways for these near periodic values to arise as we can devolve a period value through any of combination of the inverses of the functions f_1 and f_2. It means that there are many initial values of u which while not initially periodic will settle down after a time to a periodic value.

6.8 Summary

We have found that there are certain initial values of u which make it periodic and that these periodic values are solutions of quadratic equations which can be shown to generate fractals when plotted by their coefficients. We tried several different techniques but were unable to find exactly what set of quadratics yielded these polynomials, but we have found a way to generate them via matrices which are quite elegantly associated with the Fibonacci numbers. While there are an infinite number of these periodic and near periodic values of u, it would appear that there are infinitely more non-periodic values. While the periodicity of the parameter u does not mean that the parameters p_i are periodic as although the set will have the same values when u returns to its initial value, they may correspond to different directions depending on how the p_i have evolved in the meantime, I think it does demonstrate that the evolution of the mixmaster universe is very complicated. This complexity has been one of the major problems it has been difficult to overcome in studying the geodesics.

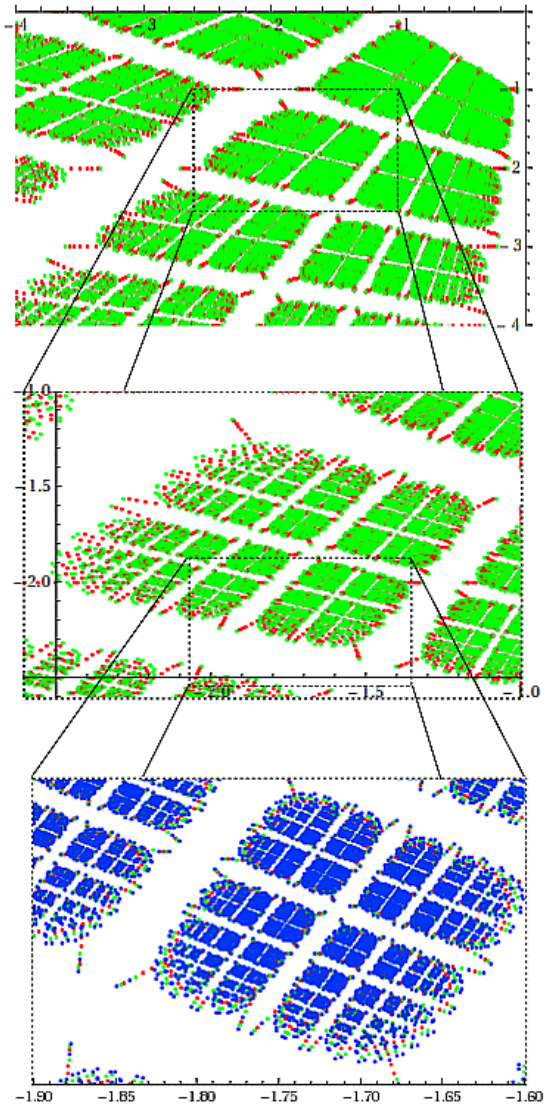

Figure 6.4: Zooming in on the two dimensional plot of quadratic coefficients demonstrates that this pattern seems to show self similarity.

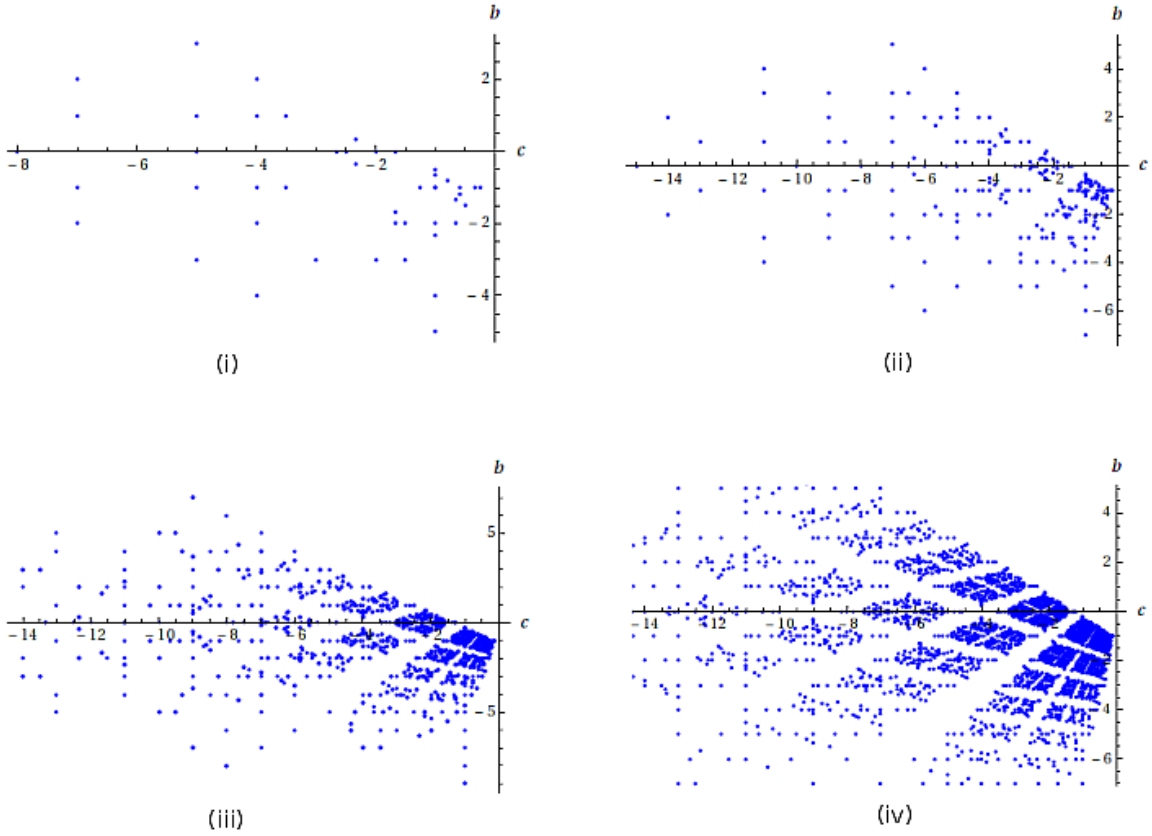

Figure 6.5: A two dimensional plot of quadratic coefficients (whose solutions give periodic values) increasing the maximum period sought as we go from (i) to (iv) showing how the fractal grows as the period increases.

Chapter 7

Discussion

In the final chapter we are going to review what has been discussed in this thesis and attempt to draw some conclusions from it. We have looked at a model of a general cosmological singularity called the mixmaster universe as a series of epochs where in each epoch the metric is that of a Kasner metric. The evolution of the mixmaster universe as a sequence of these metrics is well-described and so we constructed our mixmaster universe by pasting together Kasner metrics at a set of transition times.

The main question we have attempted to answer is whether or not it is possible in this universe to have spacelike geodesics which bounce off the singularity. This was done in the context that if it were possible, then we may be able to extract information about such a singularity via the boundary correlators in the AdS/CFT correspondence. The answer to the question proved to be more complicated than initially expected. In fact I would summarise the evolution of the answer to this question through this thesis as "yes, no, maybe yes, probably no". Naïvely from the initial study of geodesics in a pure Kasner metric in chapter 3, it seemed plausible that there was a whole region of the space of geodesics which would bounce. However, in the next chapter we demonstrated that under a certain set of transition times (logarithmically regular or shorter), then the geodesics which bounced did so very early and that it was actually impossible for them to bounce closer to the singularity than the first epoch. But on closer examination, it seemed possible for there to be a "get out clause" if the time transitions were suitably irregular.

We found in chapter five that in certain contrived situations we could get geodesics which bounced after the first Kasner epoch. However restricting our considerations to geodesics moving in one direction, it was found that even when we could have bouncing geodesics the number was pretty low. Moreover, numerical results implied that when we have more than one Kasner era, that would be catastrophic for the purely K_1 geodesics. The conclusion I would draw from all these results is that it is extremely unlikely that we have spacelike geodesics bouncing very close to the singularity. However, I am not convinced that it can be entirely ruled out although for any given geodesic in the mixmaster universe, it would have to be extremely lucky in terms of having all the epochs just the right length such that its potential manages to climb back up to zero.

One of the major difficulties to overcome in this model of the mixmaster universe is the sheer number of parameters involved in the equations being solved. Although the Kasner constants p_i evolve in a fairly straightforward way, there are still an infinite number of initial u's to choose from. Because the evolution of the p_i is very sensitive to small changes in the initial value of u, it makes drawing any definite conclusions from a small sample of such u's very difficult. When you add in the transition times and the fact that each geodesic is defined via three constants this only amplifies the problem and makes making general conclusions from finite sets of examples quite difficult. It seems that whenever a statement is made about one situation, it is possible under a different set of parameters to avoid that situation occurring.

Another problem is that because none of the equations are solvable analytically, this means we have to look to numerics to either find the maximum of the geodesic's piecewise potential or find the roots. The numerical calculations in this thesis were all done using Mathematica. Most of the problems that arose were basically a result of the potential for the geodesic being a piecewise function. Ideally to determine if a geodesic bounces, we wanted to find either the largest root or the global maximum of the potential. The problem was that these could potentially occur anywhere

along the t-axis. Guaranteeing that it had found a geodesic that bounced where it claimed it did was non-trivial. Indeed the early indication was that even in the regular time schemes geodesics could be found which bounce in later epochs (closer to the singularity), but this was later discovered to be an erroneous result caused by finding only a local maximum in the potential and that in fact, such a geodesic would have already bounced in the first Kasner epoch. Doing numerical calculations also requires that we pick numerical values for the parameters in our model and as mentioned before when this is done, it always then seems difficult to make too many generalisations about the long term behaviour.

However, it seems that the conclusions we can draw are as follows. If the time transitions occur within a geometric series $\frac{1}{r^n}$ ("regular"), it is impossible to have geodesics bouncing close to the singularity. If we try and get around this by perturbing the time transitions away from regular, it is possible to have geodesics that bounce inside the first Kasner era of our evolution but seems that when we hit the next era, we lose this bouncing. So we can only probe inside the singularity as far as the end of this first Kasner era which is determined by the integral part of initial u. This gives us a cut-off as to how close to the singularity we can get.

Chapter six is at some level completely separate to the earlier work on bouncing geodesics. In it we showed that we could find periodic values of the parameter u and that these could produce interesting pictures when visualised in the right way. Although it is difficult to see the connection to the previous work, it was included because it demonstrates in a different way that fundamentally the mixmaster universe is complicated by nature and it is this complexity which has caused the problems for the analysis of the geodesics. Another way in which it can be seen to be connected to the work on geodesics is that, many of the equations we studied in the process of understanding these geodesics, from the evolution of their constants K_i to the inequalities required for a geodesic to potentially bounce, quite heavily depended on the evolution of these parameters p_i. So the fact that chapter six shows that the evolution can be easily seen to be extremely complicated means that it is un-

derstandable that we struggled to derive many general results. It seems that in the mixmaster universe, the evolution of the parameters in the Kasner epochs massively affects many aspects of the universe including the geodesics and thus the chaotic nature of this evolution causes many difficulties in studying other aspects of the cosmology of the mixmaster universe.

It is also important to discuss the model of the mixmaster universe which was used in this research, as it was a fairly simplified model of the full mixmaster universe. Firstly, by sticking together the Kasner epochs in the way we have was justified by the fact that the transition from one epoch to the next in the mixmaster universe occurs very quickly. We have modelled this as happening instantaneously which is something of a simplification. The full picture of how a spacelike geodesic crosses from one epoch to the next could be far more complicated. Secondly, we have been using Kasner epochs within which, each t =constant hypersurface is a flat space, whereas these hypersurfaces in the mixmaster universe are not flat and this could cause even further complications in the geodesic behaviour. However, as our simplified model proved very difficult to study in much generality, it seems unlikely that introducing these further complications would simplify the calculations in any way. As we have been unable to completely rule out the bouncing of geodesics off the singularity, studying a more complex model of this cosmology could be an interesting future area of research.

To summarise, we have tried to determine whether it was possible for spacelike geodesics in the mixmaster universe to bounce off the singularity with a view to using the AdS/CFT correspondence to extract information about the singularity via these geodesics. We have shown that the behaviour of the mixmaster universe is extremely complicated and makes the answer to this question uncertain. However, after many different ways of tackling this question, all the analysis seems to point to the conclusion that while potentially not impossible, such bouncing is extremely unlikely to occur.

Bibliography

[1] A. Einstein: "Grundlage der allgemeinen Relativitätstheorie", Annalen der Physik 49 (1916)

[2] J. Polchinski: String Theory (Volume 1), CUP (1998)

[3] E. Kiritsis: "String Theory in a Nutshell", Princeton University Press (2007)

[4] B. Zwiebach: "A First Course in String Theory", CUP (2004)

[5] O. Aharony, S. Gubser, J. Maldacena, H. Ooguri, Y. Oz: "Large N Field Theories, String Theory and Gravity" arXiv:hep-th/9905111v3

[6] J. Maldacena: "TASI 2003 Lectures on AdS/CFT", arXiv:hep-th/0309246v5

[7] G. T. Horowitz, J. Polchinski: "Gauge/gravity duality", arXiv:gr-qc/0602037v3

[8] G. 't Hooft: (1993), "Dimensional Reduction in quantum gravity" arXiv:gr-qc/9310026

[9] L. Susskind: J. Math. Phys 36, 6377 (1995), "The World as a Hologram", arXiv:hep-th/9409089

[10] E. Witten: Adv. Theor. Math. Phys.2 (1998), "Anti-de Sitter Space, Thermal Phase Transition, And Confinement In Gauge Theories", arXiv:hep-th/9803131v2

[11] G. Horowitz: "Introduction to Holographic Superconductors", arXiv:1002.1722v2 [hep-th]

[12] C. Herzog: J.Phys.A42:343001,2009, "Lectures on Holographic Superfluidity and Superconductivity", arXiv:0904.1975v2 [hep-th]

[13] L. Fidkowski, V. Hubeny, M. Kleban and S. Shenker: JHEP 0402, 014 (2004) arXiv:hep-th/0306170v3

[14] V. Hubeny (2004): "Probing singularities". NATO Advanced Study Institute And EC Summer School On String Theory: From Gauge Interactions To Cosmology, Cargese, France, Springer.

[15] V. Balasubramanian, S. F. Ross. Phys Rev D 61 (2000): arXiv: hep-th/9906226

[16] J. M. Maldacena: arXiv: hep-th/0106112

[17] T. S. Levi, S. F. Ross: arXiv:hep-th/0304150

[18] P. Kraus, H. Ooguri, S. Shenker: Phys. Rev. D 67, 124022 (2003) arXiv:hep-th/0212277

[19] C. W. Misner, K S Thorne, J A Wheeler: "Gravitation"

[20] I. M. Khalatnikov, E M Lifschitz: Phys Rev Letters 24 (1970): "General Cosmological Solution of the Gravitational Equations with a Singularity in Time"

[21] E. M. Lifschitz, I M Khalatnikov: Advan. Phys. 12 (1963): "Singularities of Cosmological Solutions of the Gravitational Equations"

[22] I. M. Khalatnikov, E. M. Lifschitz, V. V. Sudakov: Phys Rev Letters 6 (1961): "Singularities of the Cosmological Solutions of Gravitational Equations"

[23] C. W. Misner: Phys Rev Letters 22 (1969) "Mixmaster Universe"

[24] S. M. Carroll: "Spacetime and Geometry, An Introduction to General Relativity", Addison Wesley (2004)

[25] N. M. J. Woodhouse: "General Relativity", Springer (2007)

[26] N. J. Cornish, J. J. Levin: Phys.Rev. D55 (1997) 7489-7510: "The Mixmaster Universe: A Chaotic Farey tale", arXiv:gr-qc/9612066v1.